FINAL REPORT

MATRIX SOLUTION OF SHELLS OF ARBITRARY SHAPE SUBJECTED TO ARBITRARY DYNAMIC LOADING

A Research Project Supported by a NASA Grant in
Space-Related Sciences

NsG-518 .

Project No. DRI 626-6607-F

August 1966

UNIVERSITY OF DENVER

Final Report
626-6607-F

MATRIX SOLUTION OF SHELLS OF ARBITRARY SHAPE SUBJECTED TO ARBITRARY DYNAMIC LOADING
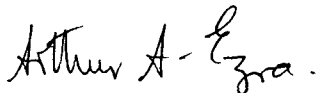
A Research Project Supported by a NASA Grant in
Space Related Sciences (NsG-518)

Submitted by

Denver Research Institute
University of Denver

Submitted to

National Aeronautics and Space Administration

August 1966

APPROVED BY:

Dr. Arthur A. Ezra
Head, Mechanics Division

PREPARED BY:

Dr. Rudolph Szilard
Professor of Civil Engineering
Senior Research Engineer

TABLE OF CONTENTS

TABLE OF CONTENTS (Cont.)

LIST OF FIGURES

LIST OF FIGURES (Cont.)

LIST OF TABLES

NOMENCLATURE

a, b	dimensions of discrete elements
c	bedding constant
A, B	matrices
$A_1, A_2 \ldots A_r$	constants
d_j	vector of edge displacements
D	flexural rigidity of plate and shell
E, E_0, E_e, E_x, E_y	moduli of elasticity
$f(t), f_1(t), f_2(t)$	function of
F_i, F_j	vectors of edge displacements
G_e	equivalent shear modulus
h, h_e	thickness of shell
i, j	indices
$k_x, k_y, k_{\bar{x}}, k_{\bar{y}}$	curvatures
k_{ij}	element stiffness matrix in X, Y, Z intermediate coordinate system
K_{ij}	stiffness matrix of total structure in general reference coordinate system
ℓ	length
m=n=1, 2, 3 . . .	numbers
$\bar{m}$	mass per unit area
m_x, m_y, m_{xy}	moments per unit length
M	mass of single degree freedom system
P_0	maximum ordinate of time dependent pressure function
p_x, p_y, p_z	surface loads in local coordinate system
p_m	circular frequency of forcing function
P_x, P_y, P_z	concentrated loads in local coordinate system
$P_{\bar{x}j}, P_{\bar{y}j}, P_{\bar{z}j}$	generalized loads at point "j" in general reference coordinate system

q_x, q_y	transverse shear per unit length
r_x, r_y	radii of curvature
R_i, R_j	generalized nodal forces at points "i" and "j" respectively
R	resistance of one degree freedom system
t	time
$[T]$	transformation matrix
$T_1, T_2, \ldots T_1$	elements of transformation matrix
$2T$	period of Fourier series expansion
u, v, w	displacement components in local coordinate system
$\overline{u}, \overline{v}, \overline{w}$	displacement components in general reference coordinate system
$_0\overline{u}_i, {}_0\overline{v}_i, {}_0\overline{w}_i$	components of eigenvectors
$\overline{U}_{im}, \overline{V}_{im}, \overline{W}_{i0}$	Fourier Series constants of deflection components in general coordinate system
$_0U_{1r}, {}_0U_{2r} \ldots$	amplitudes of eigenvectors
$U_{real}, U_{discrete}$	potential energies
V	volume
$w_0, w_1 \ldots w_r$	lateral displacements in finite difference gridwork
W_{mn}	constant of double Fourier Series expansion
x, y, z	coordinates in local coordinate system
$\overline{x}, \overline{y}, \overline{z}$	coordinates in general reference coordinate system
X, Y, Z	axes of local coordinate system
$\overline{X}, \overline{Y}, \overline{Z}$	axes of general reference coordinate system
X', Y', Z'	axes of intermediate coordinate system
X_n	amplitudes of single degree freedom system
$a_i \ldots a_r$	phase angles
a_m, β_m	frequencies in Fourier Series
$\epsilon_x, \epsilon_y, \lambda$	components of strain

δ_i	displacement vector in general reference coordinate system
$_0\delta_i$	eigenvector in general reference coordinate system
Δ_{im}	amplitude vector in general reference coordinate system
$\theta_{\overline{x}i}$, $\theta_{\overline{y}i}$, $\theta_{\overline{z}i}$	angles of rotation at node "i" in general reference coordinate system
λ	length of finite difference grid
ν	Poisson's ratio
μ_{xx}, μ_{xy}, etc.	directional cosines
π	3.14159
Π_{im}	Fourier coefficients of time dependency of generalized loads
ρ_{ij}	stiffness matrix in local coordinate system
σ, τ	stress components
ϕ	displacement function
Φ	displacement function of element
ω	natural circular frequency of free vibration
$\mathcal{W}^0_{ij}$, $\mathcal{W}_{ij}$	elements of mass matrix in local and general coordinate systems, respectively
$\mathcal{M}^0_{ij}$, $\mathcal{M}_{ij}$	mass matrix in local and general coordinate systems, respectively
$\mathcal{P}_{im}$, $\mathcal{P}_{jm}$	Fourier coefficients of the component of the generalized load in $\overline{X}$ direction
$\mathcal{R}_{im}$	Fourier coefficient of the time dependent part of the dynamic load

SYNOPSIS

12263

After a brief review of the state-of-the-art the problematics pertinent to a discrete element approach to dynamic shell problems are discussed. In the derivation of the discrete element properties using unit displacement theorem, the stiffness coefficients of a square flat shell element are developed by solving the differential equations of the theory of elasticity by finite difference methods. Symmetry in the stiffness matrix has been achieved via virtual work of the edge forces. Monotonic convergence of the solution is assured by satisfying the compatibility requirements of stresses and displacements within the element as well as along the adjoining edges. The basically different convergence criteria of small vs. large element solutions are treated. Expressing the arbitrary (in space and time) loads by Fourier series the differential equations of motions are transformed into coupled algebraic equations well suited for computer solution. The frequencies of the free vibration are obtained as eigenvalue solutions of the dynamical matrix. The accuracy of the method is checked against known analytical solutions. The procedure for automation of the solution is outlined along with the areas of future research.

Author

I.   INTRODUCTION

The modern tendency in structural engineering is characterized by the increased use of shell structures because of their inherent structural, economical and other advantages. Where complete enclosure is required as in the case of aerospace, naval structures, pressure vessels, etc., the use of shell structures is mandatory, since their remarkable load carrying capacity originating from their three-dimensional load-carrying action permits the use of lighter,thus more economical structures.

The more effective use of shells is considerably hampered by the mathematical difficulties inherent to the classical shell theories. Even in the case of static loads, solution of the differential equations of equilibrium and compatibility (except for the most elementary cases) is too complex for the average designer. These mathematical difficulties increase exponentially in case of dynamic loading, non-symmetrical geometry, arbitrary load distribution, arbitrary boundary conditions, etc., until they reach the point where the solution of the specific problem, for all practical purposes, is prohibitive or even impossible.

On the other hand, in spite of these mathematical difficulties, a great need exists to rationally design modern aerospace, civil and naval structures consisting of single and double curved shells of arbitrary shape and boundary condition subjected to arbitrary (in space and time) dynamic loading.

During recent years the development of high speed electronic computers coupled with improved matrix procedures made it possible to attack the structural dynamics problem of complex aerospace structures using discrete elements of the continuum and treating the complex structure as an assemblage of finite elements. Although, as is the case in all new developments, considerable further research effort is required to solve all problems pertinent to discrete element methods, it already can be stated that this relatively new method is able to furnish satisfactory information regarding static and dynamic stress distribution in complex structures, where the application of the classical theory of elasticity fails completely.

The key to the solution of dynamic response of shells of arbitrary shape by discrete element method is the development of suitable stiffness (or influence) coefficients of the shell elements, which describes the elastic characteristics of the structure and ensures

monotonic convergence of the solution taking into account both the membrane and bending stresses. Thus the basic objective of the research described in this report was directed toward the development of such compatible stiffness coefficients for square shell elements, first disregarding the effect of curvature.

In spite of the fact that in recent years considerable effort has been reported in the pertinent literature concerning the development of stiffness coefficients for shell elements (see References), a basically new approach has been taken herein to avoid the known shortcomings of previous solutions.[3] Furthermore, the possibility of a unique solution based on the use of "large" discrete elements vs. small ones offering considerable economy coupled with high accuracy has been discussed. The economical advantage of the large element method is evident since it reduces the order of the stiffness matrix considerably, thus eliminating partially the problems inherent to operation with large matrices resulting in savings in the required computer operation time.

The second, equally important, objective was to outline the course of further developments in the field of stiffness matrix solution of complex static and dynamic shell problems.

Considerable advantage of the discrete element method based on stiffness method approach is its versatility on one hand, and its simplicity, on the other. That is to say that basically the same method can be used regardless if the shell is single or double curved (including negative Gaussian curvature), isotropic or orthotropic, having variable thickness, and stiffness. Though considerable research is required to determine the stiffness coefficients, this work should be done only once, since its results are reusable. The same can be said about thermo stress and non-linear stress problems, etc.[4]

Furthermore, the fact that the discrete element approach uses methods familiar to structural engineers instead of those of specialized structural researchers, should not be overlooked in practical application. Similarly, no new programing is required, since standard programs available at any computer center are used underlying again the economy of the solution. This economy can be further expanded by the possibility of complete automation of the procedure.

In order to check the accuracy of the solution of the method presented, the results of various two and three dimensional stress problems have been compared with available analytical solutions.

Simultaneously, the convergence of the finite element solution to the right solution has been carefully established.

Although attention has been concentrated on flat thin plate elements, the consideration of the effect of curvature in the discrete elements has been also briefly investigated.

Arbitrary, in space and time, dynamic loads can be treated by matrix approach with relative ease, since assigning concentrated forces to the node points and expressing their time dependency in the form of Fourier series transforms the differential equation of motion into coupled algebraic equations which are well suited for computer solution. The importance of the use of dynamically equivalent mass matrix, if high accuracy is required or if large element approach is used, has been established in this research.

II.   BRIEF REVIEW OF THE STATE-OF-THE-ART

The classical solutions of the dynamics of shells follow the well-traveled path outlined by Love[5] and Flügge.[1,6] Such solution, except in the simplest case, is prohibitive due to the mathematical difficulties involved.

The finite difference method coupled with relaxation procedure provides a far more versatile method than the classical solution,[7] but in most of the cases, the differential equations of motions of shells of arbitrary shape cannot be derived, thus the finite difference solution is limited to classical problems.[2,7] Further complications arise in consideration of arbitrary boundary conditions such as partial elastic supports, etc.

The energy methods in form of: 1) conservation of energy, 2) virtual work, 3) minimum potential energy, and 4) complimentary energy are powerful tools, but they do not lend themselves to easy computer use.[8]

Hrennikoff[9] replaced the continuous material of elastic body by a frame work of bars arranged to a definite pattern. The impetus to Hrennikoff discrete element solution was given by the invention of high speed electronic computers. Pioneering work in developing the displacement method using stiffness matrix formulation (direct stiffness method) is due to Turner, Clough and Martin,[10] who replaced two and three dimensional structures by an assemblage of plates and beams and of other basic structural elements.

Argyris[11] introduced the "force method," which represents the expansion of the classical solution of statically indeterminate structures. The stiffness and force method can be formulated in completely parallel form.

The combination of above discussed discrete element methods is "the displacement" method based on the use of flexibility matrix.[12] Among other things the argument in favor of the use of stiffness matrices is that it saves considerable amount of computing time and storage allocation.

Although discrete element methods for solution of complex static and dynamic stress problems require considerable further research efforts, they hold great promise for economic solution of

complex stress problems. One part of the improvements should come from introduction of more realistic representation of the continuum by discrete elements, while the other equally important improvement should come from computer designers in the form of larger and more powerful computers.

III. DISCRETE ELEMENT METHODS AND THEIR CONVERGENCE
CRITERIA

Matrix solutions of static and dynamic stress problems require by their nature the discretization of the continuum into finite number of elements. The equilibrium and continuity of displacement are expressed at the node points. The representation of continua by discontinua is common to all discrete element methods.

The most important finite element methods presently used are:

1. Displacement method using stiffness matrices (direct stiffness method)

2. Displacement method using flexibility matrices

3. Force method (Argyris)

4. Method of transfer matrices

5. Klein's method

In all of these methods the investigation of the convergence of the solution to the correct value is of basic importance. Although this report deals only with "direct stiffness method", the following discussion concerning convergence criteria is common to all discrete element methods. [13, 14]

Mathematically, the discrete element representation of continuum in the linear elastic range, strongly resembles the "Ritz method" used in solution of various stress problems in the theory of elasticity, i.e., the true displacement state of the structure is represented only approximately by the displacements of the discrete elements, consequently the most general criterium of convergence of the discrete element solution is the equality of the potential energy of the real system (U_r) and that of the substitute system, obtained by assembling "n" discrete elements; thus

$$U_{real} = \sum_{1}^{n} U_{discrete,} \tag{1}$$

or considering the work of the external loads, equation (1) can be written as

$$\delta(\overline{x}, \overline{y}, \overline{z}, t)\, p(\overline{x}, \overline{y}, \overline{z}, t) = \sum_{i=1}^{n} \phi_i(\overline{x}, \overline{y}, \overline{z})\, P_i(\overline{x}, \overline{y}, \overline{z}, t), \qquad (1a)$$

where δ is the total displacement vector of the whole structure and ϕ_i defines the distortion of the structure due to unit load of coordinate "i" and P_i is the generalized load vector at coordinate "i" in system $\overline{X}$, $\overline{Y}$, $\overline{Z}$.

From equations (1) and (1a) follows that a similarity between the final deformation of the discrete elements and that of the corresponding region of the real structure must be maintained. Thus, all possible motions (translations and rotations) of the node points must be considered.

Furthermore, the deformation of the elements between node points must also satisfy equations (1) and (1a); consequently, the displacements within the discrete element must be similar to those of the corresponding part of the real structure.

Since stresses and strains are compatible and continuous within the continuum, compatibility of all stress and displacements within the element and at the edges between adjacent elements must be maintained, which is another important requirement to obtain convergence to the exact solution.

Additional convergence criteria particular to direct stiffness matrix approach to dynamics of shells used in this report, will be discussed in Section VII.

The accuracy of the discrete element solution depends also upon how well the discrete element idealizes the real continuum. In the idealization of shell structures presented herein, flat square elements are used (Figure 1), which will be subjected to stretching and bending. Flat triangular elements are superior to rectangular ones in case of idealization of shells of arbitrary geometry, (Figure 2), but the mathematical difficulties in obtaining stiffness coefficients for triangular elements using the method applied in this report are considerably greater, thus the development of stiffness coefficients for "compatible" triangular discrete elements is left to future investigations. A simple transformation of moderately tapered trapezoid elements into equivalent square elements has been developed to extend the usability of the square elements.
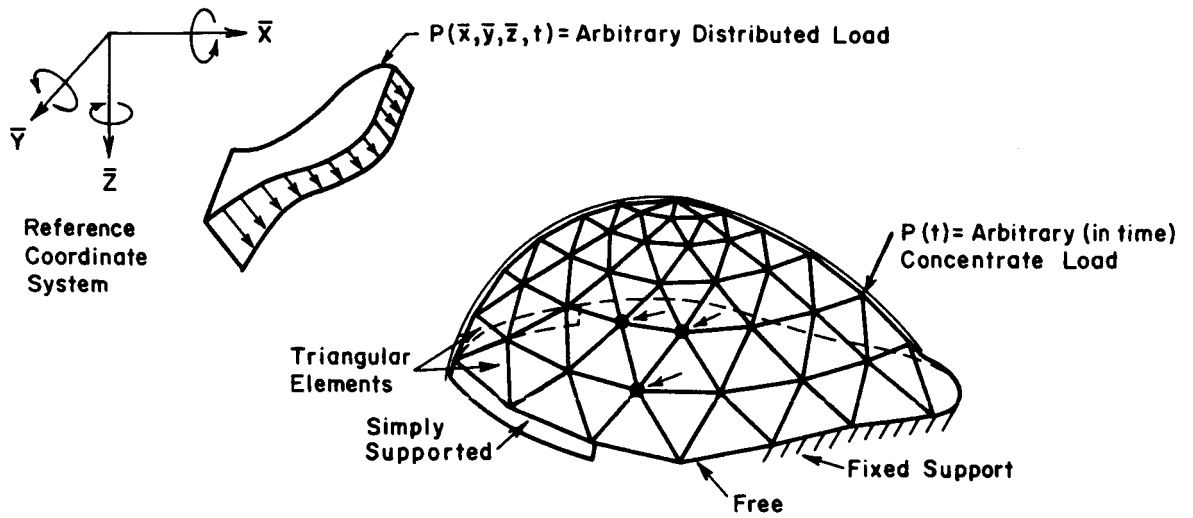
Figure 1. Shell of Arbitrary Shape
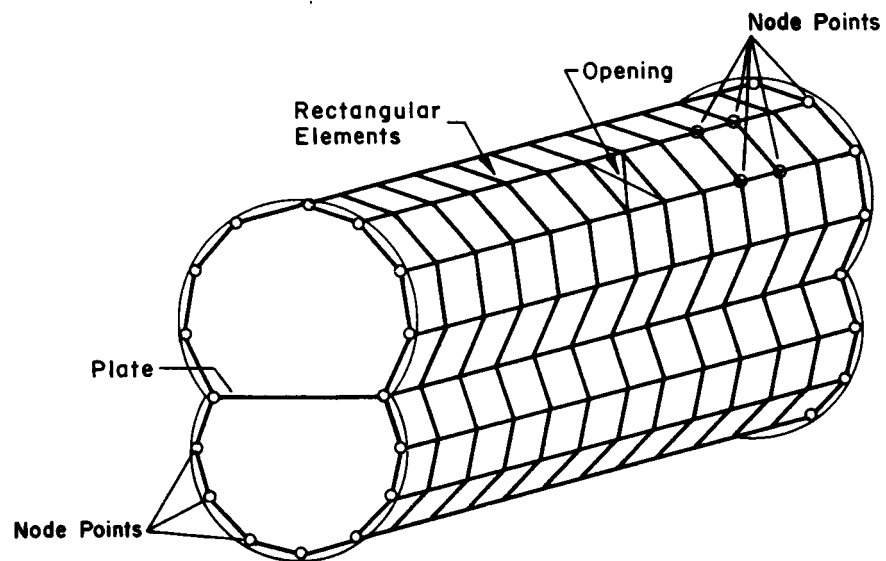
Figure 2. Cylindrical Shell of Arbitrary Shape (Fuselage)

Flat element representation of curved shell automatically violates the continuity of slope requirement along the edges of adjacent elements. Folded plate idealization of cylindrical shells, however, has indicated in more conventional approaches, [15] that such an idealization is permissible, especially in case of static shell problems, and by increasing the number of discrete elements, the solution converges to the exact one.

If the shell is relatively flat or the subdivision is relatively small, arbitrary shell surfaces can be also well approximated by rectangular discrete elements. By the introduction of double curved elements the geometrical fitting problem is considerably reduced.

Especially in case of dynamic problems, the proper load representation, including that of inertia forces may effect the convergence of the solution, i.e., the results of discrete element approaches, converge but not to the exact solution. Thus the generalized forces applied at the node points must satisfy certain energy requirements which will be discussed later in detail.

Finally, the accuracy of the solution can be adversely effected by computer errors inherent to operations with large matrices (See Section X). Since direct stiffness method yields well conditioned, symmetric, positive-definite matrices in band matrix form, in the author's opinion, this approach is more suitable to handle complex dynamic problems of arbitrary shells than others previously discussed. In addition, the ease with which any physically possible boundary condition can be handled, [16] should not be overlooked.

IV. DYNAMIC ANALYSIS OF SHELLS BY DISPLACEMENT METHOD

The differential equation of undamped motion of any structure, including shells of arbitrary shape, can be written in matrix form:

$$\{\delta_i(t)\} + [K_{ij}]^{-1}\{ \mathfrak{M}_{ij}\ \ddot{\delta}_j(t)\} = [K_{ij}]^{-1}\{P_j(t)\}, \tag{2}$$

where δ_i represents the vector of nodal displacements in a general orthogonal reference coordinate system $\overline{X},\ \overline{Y},\ \overline{Z}$ (Figures 1 and 2):

$$\delta_i(t) = \begin{Bmatrix} \overline{u}_i(t) \\ \overline{v}_i(t) \\ \overline{w}_i(t) \\ \theta_{\overline{x}i}(t) \\ \theta_{\overline{y}i}(t) \\ \theta_{\overline{z}i}(t) \end{Bmatrix}, \quad i = 1,\ 2,\ 3\ \ldots \tag{3}$$

and $P_j(t)$ represents the vector of nodal forces in the same coordinate system

$$P_j(t) = \begin{Bmatrix} P_{\overline{x}y}(t) \\ P_{\overline{y}j}(t) \\ P_{\overline{z}i}(t) \\ M_{\overline{x}j}(t) \\ M_{\overline{y}j}(t) \\ M_{\overline{z}j}(t) \end{Bmatrix}. \tag{4}$$

Furthermore, $[K_{ij}]$ is the square matrix of stiffness coefficients of the total structure, expressed again in the general reference coordinate system, and $[\mathfrak{M}_{ij}]$ is the mass matrix. The two dots in equation (2) indicate the second derivative with respect to time. Matrix $\{\mathfrak{M}_{ij}\ \ddot{\delta}_j(t)\}$ represents the inertia forces. Because of its importance in solution of dynamic stress problems in shells of arbitrary shape, it will be treated in more detail in Section VIII.

In case of free vibration, the forcing function $P_j(t)$ is zero, thus equation (2) becomes

$$\{_0\delta_i(t)\} + [K_{ij}]^{-1} \{\mathcal{M}_{ij} \, _0\ddot{\delta}_j\} = 0. \tag{5}$$

Let us assume that the stiffness and mass matrices are already known. We investigate the solution of the homogeneous differential equation (5) in the form of

$$\left.\begin{array}{l}
\{_0\overline{u}_i\} = \{_0\overline{U}_i\} \, \sin(\omega t + a_i) \\[2mm]
\{_0\overline{v}_i\} = \{_0\overline{V}_i\} \, \sin(\omega t + a_i) \\[2mm]
\{_0\overline{w}_i\} = \{_0\overline{W}_i\} \, \sin(\omega t + a_i) \\[2mm]
\quad \cdot \quad \cdot \quad \cdot \quad \cdot \quad \cdot \quad \cdot \quad \cdot \quad \cdot \\[2mm]
\quad \cdot \quad \cdot \quad \cdot \quad \cdot \quad \cdot \quad \cdot \quad \cdot \quad \cdot
\end{array}\right\} \tag{6}$$

where $\{_0\overline{U}_i\}$, $\{_0\overline{V}_i\}$, $\{_0\overline{W}_i\}$ are column matrices of the amplitudes, ω is the "natural" angular frequency of the free oscillation and a_i is an arbitrary phase angle.

Substituting Equation (6) into (5) and performing certain matrix operation we obtain:

$$[A]^{-1} - \lambda[I] = 0, \tag{7}$$

where $[I]$ is the identity matrix, and

$$\lambda = \omega^2. \tag{8}$$

Matrix $[A]$ is the "dynamical matrix"[17] of order "r" obtained from:

$$[A] = [K_{ij}]^{-1} [\mathcal{M}_{ij}]. \tag{9}$$

The inverse of the "dynamical matrix" is:

$$[A]^{-1} = [\mathcal{M}_{ij}]^{-1} [K_{ij}]. \tag{10}$$

Equation (7) represents the classical eigenvalue problem of matrix algebra[18] the solution of which is readily obtainable by standard computer programs, if the order of matrix is not excessively large.

Usually the general solution of the homogeneous matrix equation (7) is not of interest. The required information for practical purposes consists of natural frequencies and natural modes of the free oscillation

$$
\left\{
\begin{aligned}
\{_0\overline{u}_{ir}\} &=
\begin{Bmatrix}
_0\overline{U}_{1r} \\
_0\overline{U}_{2r} \\
\cdot \\
\cdot \\
\cdot \\
_0\overline{U}_{nr}
\end{Bmatrix}
\times \sin(\omega_r t + a_r), \\[2em]
\{_0\overline{v}_{ir}\} &=
\begin{Bmatrix}
_0\overline{V}_{1r} \\
_0\overline{V}_{2r} \\
\cdot \\
\cdot \\
\cdot \\
_0\overline{V}_{nr}
\end{Bmatrix}
\times \sin(\omega_r t + a_r). \\[2em]
\{_0\overline{w}_{ir}\} &=
\begin{Bmatrix}
_0\overline{W}_{1r} \\
_0\overline{W}_{2r} \\
\cdot \\
\cdot \\
\cdot \\
_0\overline{W}_{nr}
\end{Bmatrix}
\times \sin(\omega_r t + a_r)
\end{aligned}
\right\}
\tag{11}
$$

For obtaining the eigenvectors (11) pertinent to "r" eigenvalues again standard programs are available at any larger computer center. The problems involved in computing eigenvalues and eigenvectors of large dynamical matrices are treated later in detail.

To determine the displacement components produced by forced vibration Navier's solution is applied, which transforms the differential equation of the undamped vibration (2) into coupled algebraic equations. In order to achieve this highly desirable transformation, it is required that both the forcing and displacement function have the same type of time dependency.

Thus if the arbitrary time dependency of the concentrated nodal force is expressed as:

$$\{P_i(t)\} = \sum_m \left\{ \Pi_{im} \right\} \sin p_m t, \tag{12}$$

then the displacement vector must have similar expression:

$$\{\delta_i(t)\} = \sum_m \left\{ \Delta_{im} \right\} \sin p_m t, \tag{13}$$

or taking, for instance, the components of both vectors in the $\overline{X}$ direction , equations (12) and (13) can be written as:

$$\{P_{\overline{x}i}(t)\} = \sum_m \left\{ \mathcal{P}_{im} \right\} \sin p_m t, \tag{12a}$$

and

$$\{\overline{u}_i\} = \sum_m \{\overline{U}_{im}\} \sin p_m t. \tag{13b}$$

Similar expressions can be written for the other components of the force and displacement vectors. The determination of the constant $\mathcal{P}_{im}$ in case of arbitrary loads will be discussed in Section VIII.

Substituting (12a) and (12b) into the differential equation of motion and canceling the trignometric factor which appears in all terms, coupled algebraic equations, for any specific m value, are obtained:

$$\{\overline{U}_{im}\} - p^2_m [K_{ij}]^{-1} [\mathcal{M}_{ij}] \{\overline{U}_{im}\} = [K_{ij}]^{-1} \{ \mathcal{P}_{jm}\}, \tag{2a}$$

from which the only unknowns $\{\overline{U}_{im}\}$ representing the amplitudes of the displacement component can be readily obtained, since computers are extremely well suited for solution of coupled algebraic equations.

Substituting $\overline{U}_{im}$ into equation (12b) and carrying out the summation, the displacement vector in function of time in the $\overline{X}$ direction is obtained. Similar procedure is followed for the other displacement components.

Knowing the displacements $\overline{u}$, $\overline{v}$ and $\overline{w}$ at each point, the internal forces and stresses are obtained from the classical shell theory[19, 20] (Figure 3):

$$m_x = -D\left(\frac{\partial^2 \overline{w}}{\partial \overline{x}^2} + v \frac{\partial^2 \overline{w}}{\partial \overline{y}^2}\right)$$

$$m_y = -D\left(\frac{\partial^2 \overline{w}}{\partial \overline{y}^2} + v \frac{\partial^2 \overline{w}}{\partial \overline{x}^2}\right)$$

$$m_{xy} = -D(1 - v)\frac{\partial^2 \overline{w}}{\partial x \partial y} = m_{yx}$$

$$q_x = -D \frac{\partial}{\partial x} \nabla^2 \overline{w}$$

$$q_y = -D \frac{\partial}{\partial y} \nabla^2 \overline{w}$$

$$n_x = \frac{Eh}{1-v^2}\left[\frac{\partial \overline{u}}{\partial \overline{x}} + v \frac{\partial \overline{v}}{\partial \overline{y}} - (k_{\overline{x}} + v k_{\overline{y}})\overline{w}\right]$$

$$n_y = \frac{Eh}{1-v^2}\left[\frac{\partial \overline{v}}{\partial \overline{y}} + v \frac{\partial \overline{u}}{\partial \overline{x}} - (k_{\overline{y}} + v k_{\overline{x}})\overline{w}\right]$$

$$n_{xy} = n_{yx} = \frac{Eh}{2(1+v)}\left[\frac{\partial \overline{u}}{\partial \overline{y}} + \frac{\partial \overline{v}}{\partial \overline{x}}\right],$$

$$\left. \right\} \quad (14)$$

where E is the modulus of elasticity, v is the Poisson's ratio, D is the flexural rigidity[19, 20] and h the shell thickness $k_{\overline{x}} = \frac{1}{R_{\overline{x}}}$, $k_{\overline{y}} = \frac{1}{R_{\overline{y}}}$

represent the curvature in $\overline{X}$ and $\overline{Y}$ directions respectively (Figure 3). Equations (14) are conveniently solved by finite difference[7] representation of the first and second derivatives using computers again.

The key to the solution of the dynamic response of shells of arbitrary shape is the determination of the stiffness matrix $[K_{ij}]$ of the total structure. In addition to the already mentioned advantages of the direct matrix approach is the ease with which the stiffness matrix of the complete structure can be obtained from the element stiffness matrices ρ_{ij}.
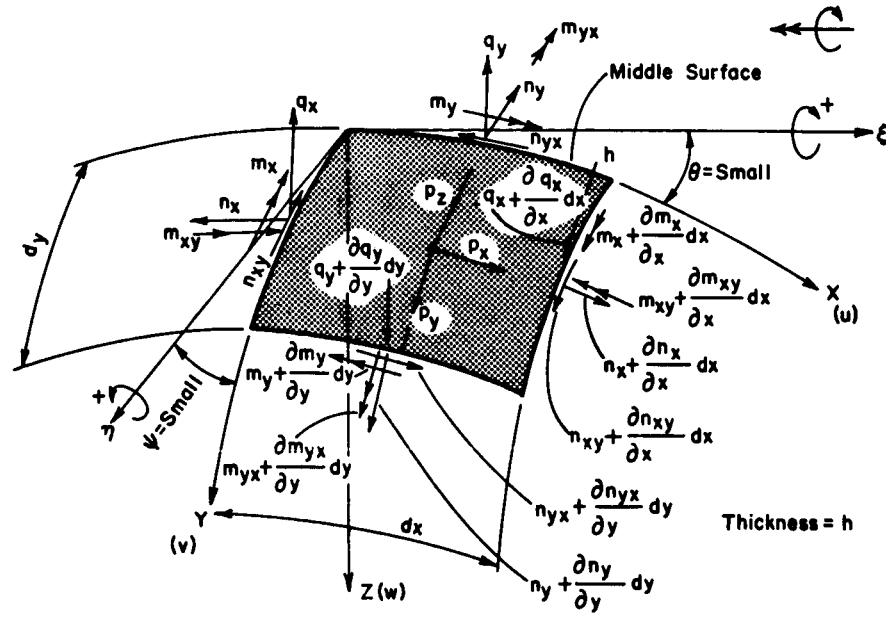
Figure 3. Infinetesimal Double-Curved Shell Element

(b.)
Reference Coordinate System of the
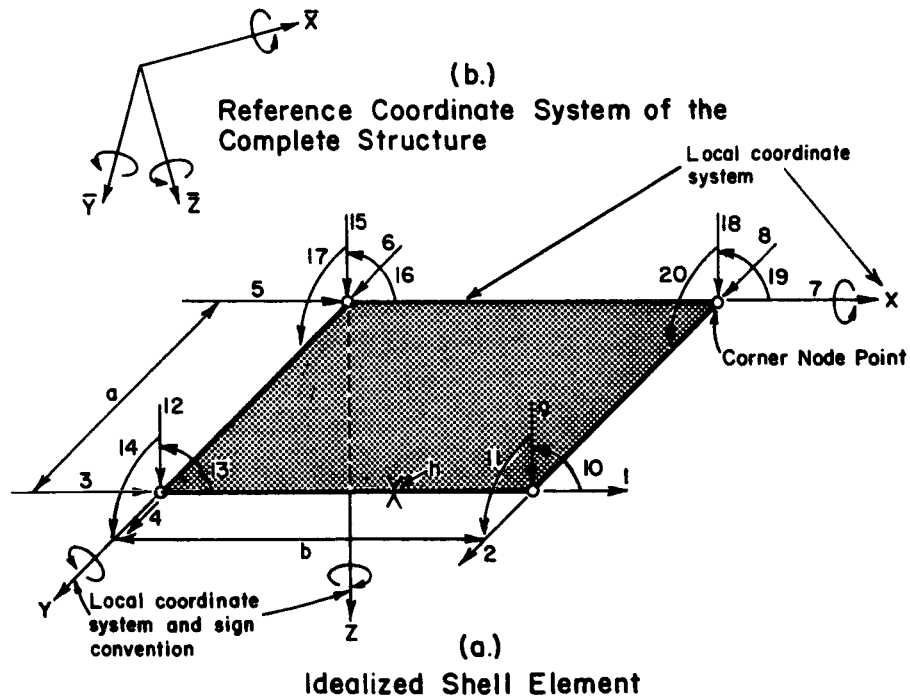**Complete Structure**

(a.)
Idealized Shell Element

Figure 4. Discrete Element

Let us assume that the element stiffness matrix $[\rho_{ij}]$ in its local coordinate system is X, Y, Z (Figure 4) has been already determined. (For determination $[\rho_{ij}]$ see Sections VI and VII). In order to express the element stiffness coefficients in the general reference coordinate system, first, a coordinate rotation is required. That is to say, the local coordinate system X, Y, Z of each element will be rotated into a parallel position with the reference coordinate system $\overline{X}$, $\overline{Y}$, $\overline{Z}$ of the total structure. This can be readily accomplished by the following matrix operation[13, 21]:

$$[k_{ij}] = [T]^{-1} [\rho_{ij}] [T], \tag{15}$$

or since it is an orthogonal transformation, equation (15) can be written as

$$[k_{ij}] = [T]^{T} [\rho_{ij}] [T], \tag{15a}$$

where $[k_{ij}]$ is the element stiffness matrix in X', Y', Z' coordinate system (Figure 5), $[T]$ is a transform matrix containing the directional cosines (Figure 5):

$$
\lceil T \rfloor =
\begin{bmatrix}
T_1 & & & & \\
& T_2 & & 0 & \\
& & T_i & & \\
& 0 & & & \\
& & & & T_n
\end{bmatrix}
\tag{16}
$$

where subscripts n = 1, 2, 3, ... represent the number of node points of the element (which is in our case n = 1, 2, 3, 4), and

$$
T_i =
\begin{bmatrix}
\mu_{xx'} & \mu_{xy'} & \mu_{xz'} & 0 & 0 & 0 \\
\mu_{yx'} & \mu_{yy'} & \mu_{zz'} & 0 & 0 & 0 \\
\mu_{zx'} & \mu_{zy'} & \mu_{zz'} & 0 & 0 & 0 \\
0 & 0 & 0 & \mu_{xx'} & \mu_{xx'} & \mu_{xz'} \\
0 & 0 & 0 & \mu_{yx'} & \mu_{yy'} & \mu_{yz'} \\
0 & 0 & 0 & \mu_{zx'} & \mu_{zy'} & \mu_{zz'}
\end{bmatrix}
\tag{16a}
$$

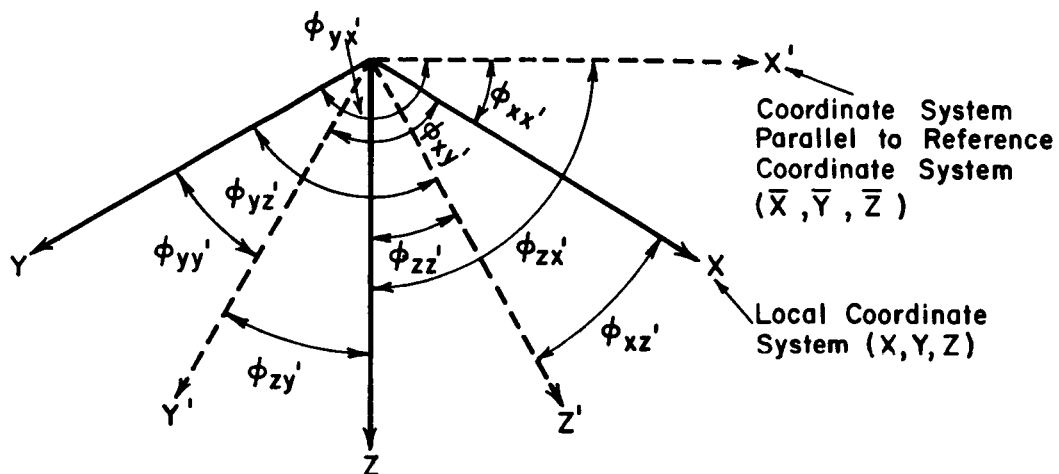where the subscripts refer to the corresponding coordinate axis as shown in Figure 5.

Figure 5. Rotation of Coordinate System
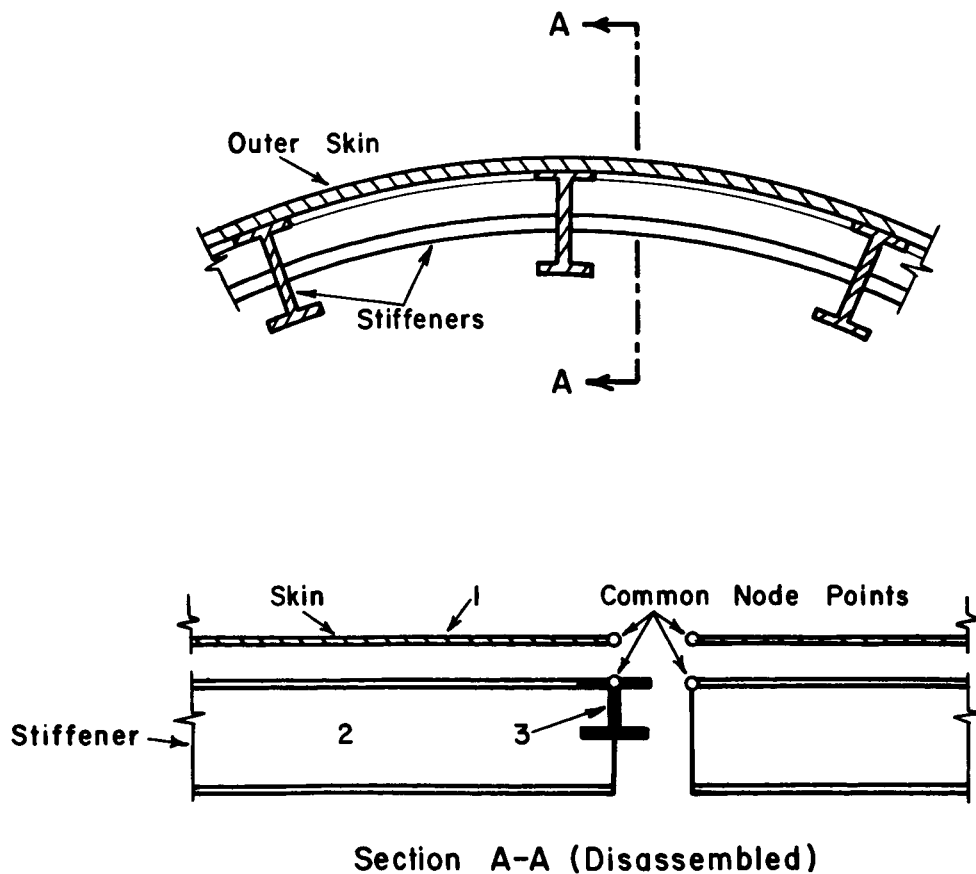

Section A-A (Disassembled)

Figure 6. Large Stiffeners

The stiffness matrix of the total structure is obtained by algebraic addition of the overlapping stiffness coefficients of the elements. Since for even a relatively small shell, the order of the stiffness matrix is quite high, automation in compiling the stiffness matrix is a must, which is discussed in Section X.

It is expedient to take care of the boundary conditions of the individual elements before compiling the stiffness matrix $[K_{ij}]$. If any motion at any node point is prevented by the support, the corresponding rows and columns of the element stiffness matrix must be deleted. Failing to do so the resulting matrix is singular, and consequently cannot be inverted.

Similar is the situation with flight structures if all rigid body motions at all node points are permitted. In order to avoid the singularity of the stiffness matrices of flight structures, artificial supports must be introduced at certain points.

Equally simple is the treatment of elastic supports (Figure 6), since it is merely required to add algebraically the stiffness factor of the elastic support to the corresponding stiffness element of the discrete element:

$$\rho_{ij} = \rho_{ij}^{(1)} + \rho_{ij}^{(2)} + \rho_{ij}^{(3)} + \ldots \ldots \tag{17}$$

Orthotropic shells (Figure 6), if the orthotropy is caused by corrugation or by small stiffeners, can be transformed into isotropic shells as follows:[22, 23]

$$G_e = \frac{E_e}{2(1+\nu_e)} = \frac{\sqrt{E_x E_y}}{2[1+\sqrt{\nu_x \nu_y}]} , \tag{18}$$

where subscripts x and y and e refer to the elastic properties in X and Y directions and to those of the equivalent shell, respectively.

Layered shells (Figure 7b) formed by curved "sandwich" panels can be handled approximately in a similar manner, that is to say, first an equivalent shell thickness is determined in X and Y direction as follows:
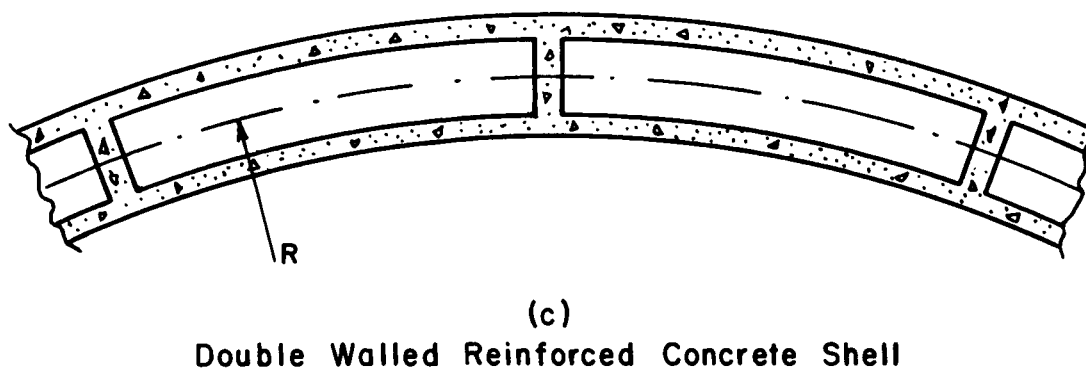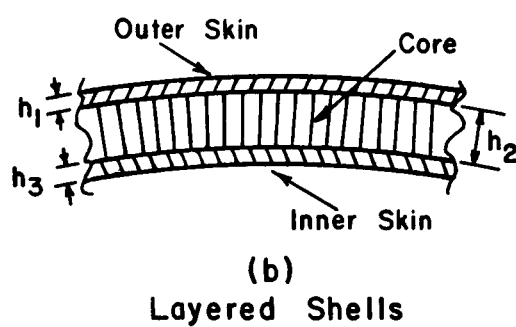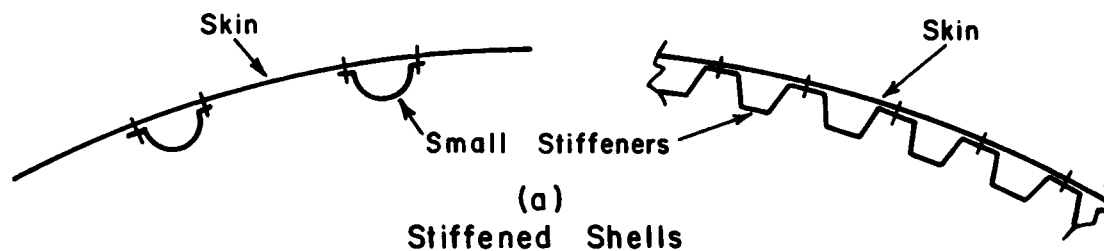
(a)
Stiffened Shells

(b)
Layered Shells

(c)
Double Walled Reinforced Concrete Shell

Figure 7. Orthotropic Shells

$$h_e = \sum_n \frac{E}{E_o} \, h \quad \text{(per unit width)},$$

$$n = 1, \ 2, \ 3 \ . \ . \ . \ . \ .$$

(19)

where E_o represents the reference modulus of elasticity, from which an equivalent moment of inertia can be easily derived; more exact ways in handling thick layered and built-up shells can be found in the pertinent literature. [24, 25]

The sign conventions for translations, rotations and for the conjugate forces and moments used in this report are shown in Figure 4 for local and for general reference coordinate systems.

The stiffness coefficients of beams and bulkheads are obtainable from the literature. [14, 21]

V.   SMALL VS. LARGE ELEMENT BEHAVIORS

The problems inherent to operations with large matrices, especially in dynamics of shells, might be considered as a serious limitation of discrete element methods using large numbers of small elements to obtain an answer which has $\pm 5\% \rightarrow 10\%$ discrepancy in comparison with the "exact" solutions.

Although considerable developments are expected in the future in computer design as well as in matrix analysis, in the coming 10 to 15 years there will be a pronounced need for drastic reduction of the size of the "dynamical matrix." The use of a symmetry[24] and the method of substructures[26, 27] are among the most widely known methods, at the present, to achieve this objective.

Szilard[28] has proved that the use of properly derived "large element" stiffness matrices reduce the order of the stiffness matrix of the total structure drastically. With a small number of large elements the same accuracy can be obtained as with a large number of small elements thus the economy of the use of large elements is evident (Figure 8). In the derivation of large element stiffness matrices no prescribed deflection pattern is forced on the edges as is the case in small element behavior, (Sections VI and VII) but unit motions (translations and rotations) are introduced at a node points of the shell element while holding the other node points fixed. The compatibility of stresses and strains within the element and at the edges is obtained by solution of the corresponding differential equations of the theory of elasticity.

It is interesting to note that the convergence characteristics of the large element approach are opposite to those of small element approaches as shown in Figure 9. There is an optimum large element size which results in the best accuracy with the smallest number of discrete elements, the analytical determination of which requires extended future research.
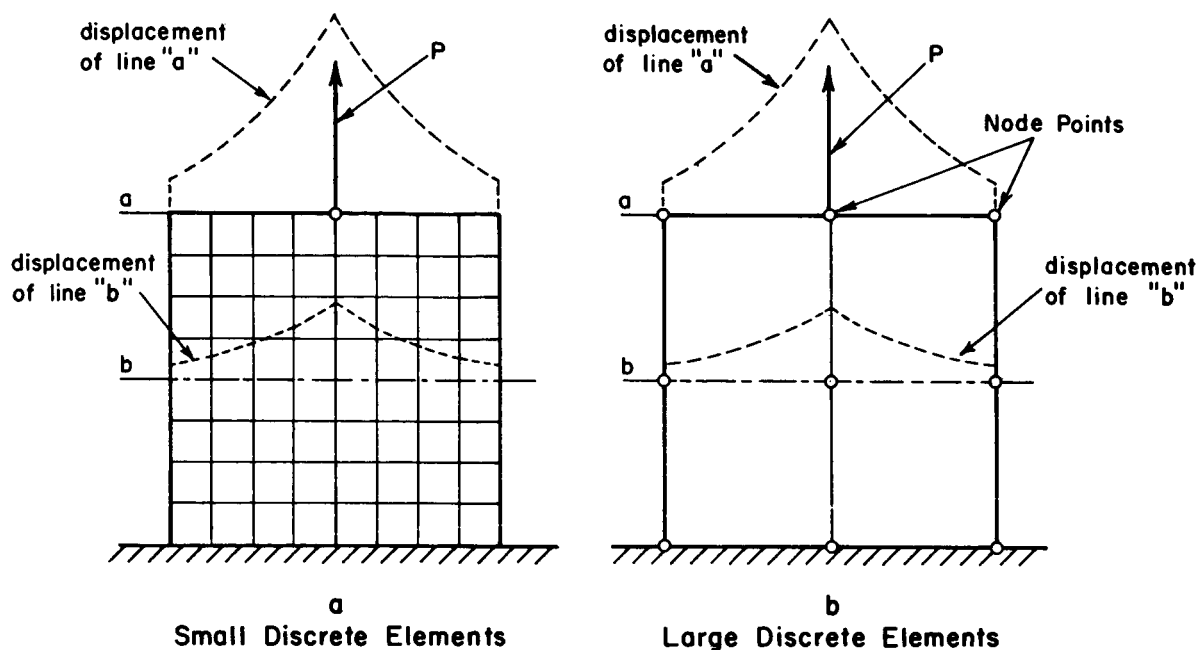
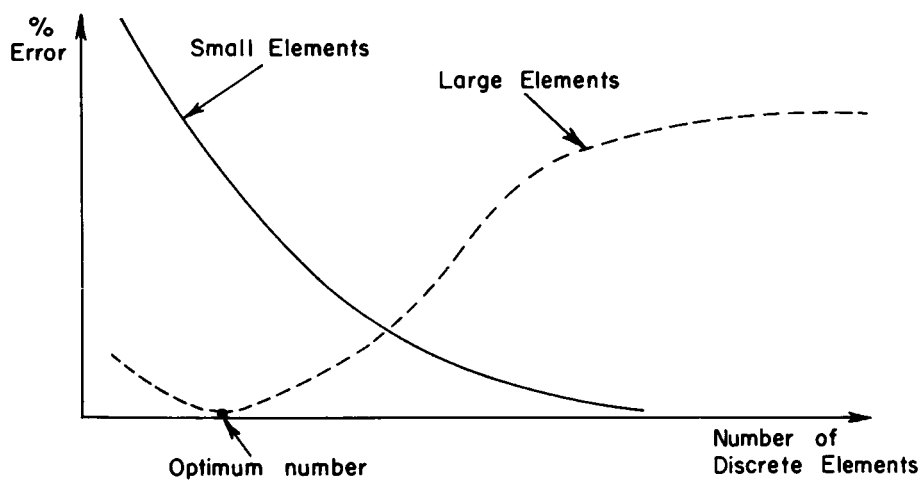Figure 8. Solution of a Stress Problem by Small and Large Discrete Elements

Figure 9. Convergence Characteristics of Small and Large Element Solutions

VI.   DERIVATION OF THE MEMBRANE PART OF STIFFNESS COEFFICIENTS

Although a survey of the literature[8, 13] indicates the availability of stiffness matrices produced by stretching or bending the flat plate discrete element, most of them violate either the compatibility of stresses, or displacements, or both. In the following, a new method which assures complete compatibility, is given considering small element behavior. Basically the same approach can be used for large discrete elements[28] and for double curved elements.[24]

Considering small element behavior the stiffness coefficients, expressed in a conveniently located local coordinate system (Figure 4), are obtained by prescribing certain edge displacements or edge stresses which result in motion (one motion at a time) of one node point while the other node points are held fixed. The active and reactive forces (and moments) assigned to the node points yield the coefficients p_{ij} of the stiffness matrix of the element in the local coordinate system.

In this report displacement functions will be assigned to edges, thus the discrete element is called a displacement model resulting in lower bound approaches to the solution of static and dynamic stress problems.

In addition to the general requirements concerning convergence, which were discussed already in Section III the following specific requirements apply:

a)   The first critical phase is the selection of suitable edge displacement functions, which assures monotonic convergence to the exact solution as finer subdivisions are used. The in-plane loading of a two dimensional continuum with a concentrated force results in an exponential type deflection curve,[28] which in a small region can be well approximated by straight lines, satisfying the general energy requirements ((1) and (1a)) of the discrete element solution; i.e., the potential energy of the original and the assembled structures will be the same if the number of subdivisions approaches infinity.

b)   The second critical step concerns the method used in evaluating the edge displacements.

c)   The third concerns the assignment of edge forces to node points so that the resulting stiffness matrix is symmetrical.

In order to assure complete compatibility of displacements and stresses within the element the differential equations of equilibrium of shallow shells (Figure 3) in function of the three displacement components have been derived:

$$
\left.\begin{aligned}
&\frac{\partial^2 u}{\partial x^2} + \frac{1-\nu}{2}\frac{\partial^2 u}{\partial y^2} + \frac{1+\nu}{2}\frac{\partial^2 v}{\partial x \partial y} - (k_x + \nu k_y)\frac{\partial w}{\partial x} = -\frac{(1-\nu^2)}{Eh}\,p_x \\[2mm]
&\frac{\partial^2 v}{\partial y^2} + \frac{1-\nu}{2}\frac{\partial^2 v}{\partial x^2} + \frac{1+\nu}{2}\frac{\partial^2 u}{\partial x \partial y} - (k_y + \nu k_x)\frac{\partial w}{\partial y} = -\frac{(1-\nu^2)}{Eh}\,p_y \\[2mm]
&-(k_x + \nu k_y)\frac{\partial u}{\partial x} - (k_y + \nu k_x)\frac{\partial v}{\partial y} + (k_x{}^2 + k_y{}^2 + 2\nu k_x k_y)\,w\ + \\[2mm]
&+ \frac{h^2}{12}\nabla^4 w = \frac{p_z}{Eh}\,(1-\nu^2)\ ,
\end{aligned}\right\}
\tag{20}
$$

where k_x and k_y are the curvatures in X and Y directions, respectively.

Since for the idealization of the shell elements used in this report flat discrete elements have been assumed ($k_x = 0$ and $k_y = 0$), the resulting three differential equations of equilibrium are partially uncoupled yielding:

$$
\left.\begin{aligned}
&\frac{\partial^2 u}{\partial x^2} + \frac{1-\nu}{2}\frac{\partial^2 u}{\partial y^2} + \frac{1+\nu}{2}\frac{\partial^2 v}{\partial x \partial y} = -\frac{(1-\nu^2)}{Eh}\,p_x\ , \\[2mm]
&\frac{\partial^2 v}{\partial y^2} + \frac{1-\nu}{2}\frac{\partial^2 v}{\partial x^2} + \frac{1+\nu}{2}\frac{\partial^2 u}{\partial x \partial y} = -\frac{(1-\nu^2)}{Eh}\,p_y
\end{aligned}\right\}
\tag{21}
$$

and

$$
D\nabla^4 w = p_z\ ,
\tag{22}
$$

where

$$
D = \frac{Eh^3}{12(1-\nu^2)}
\tag{23}
$$

represents the flexural rigidity of the shell or plate.[19]

Equation (21) is the differential equation of equilibrium of the two dimensional stress problems, while equation (22) represents the well known plate equation[19] derived by Kirchoff.

By solving the differential equations of the two dimensional stress problem[21] for prescribed straight line edge motion, the required compatibility of stresses and displacements within the element are fully satisfied.

In order to assure complete compatibility of edge displacements and edge stresses the method of images as shown in Figure 10, is introduced. Because of the material continuity not only the displacements of node points of adjoining discrete elements but the displacements along the lines connecting the node points are the same. Furthermore, by solving the differential equation of the two dimensional stress problem of the 2a × 2b element (Figure 10), the compatibility of stresses along the edges is also ensured.

In solving differential equations (21 a and b) finite difference method has been utilized. Symmetry of loading and structure could be exploited by using "guided" boundary conditions, as shown in Figure 11 corresponding to one type of motion allowed along the edge moved. For finite difference subdivision an 8 × 8 mesh size was used (Figure 11). The finite difference solution, which is symbolically shown in Figure 12 has yielded u and v displacements, from which the edge reactions have been obtained:

$$n_x = \frac{Eh}{1-\nu^2} \left(\frac{\partial u}{\partial x} + \nu \frac{\partial v}{\partial y} \right) \qquad \text{a)}$$

$$n_y = \frac{Eh}{1-\nu^2} \left(\frac{\partial v}{\partial y} + \nu \frac{\partial u}{\partial x} \right) \qquad \text{b)} \qquad (24)$$

$$n_{xy} = \frac{Eh}{2(1+\nu)} \left(\frac{\partial u}{\partial y} + \frac{\partial v}{\partial x} \right) . \qquad \text{c)}$$

Since linear edge displacements have been described singularity was not a problem in obtaining the correct solution.

The so derived distributed edge forces had to be assigned to the node points so that the resulting matrix is symmetrical. The conventionally used method which assigns statically equivalent concentrated forces and moments to the nodes works only in the simplest cases and results in an unsymmetrical stiffness matrix, which, especially in structural dynamics, creates considerably difficulties in the matrix and computer operations.
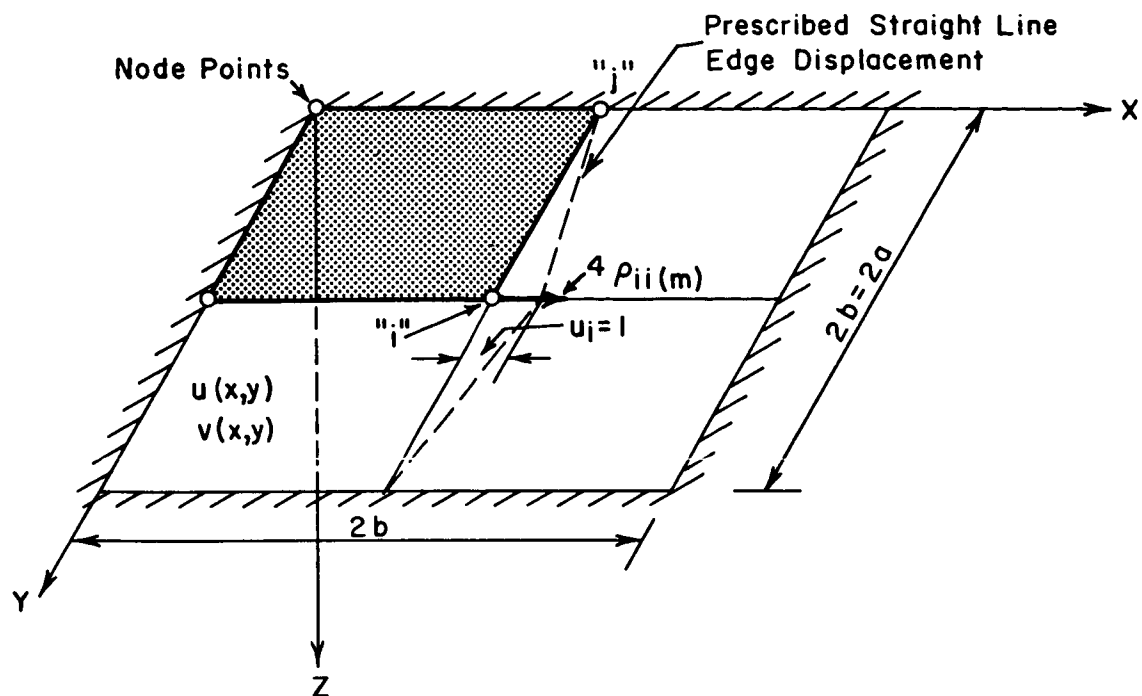
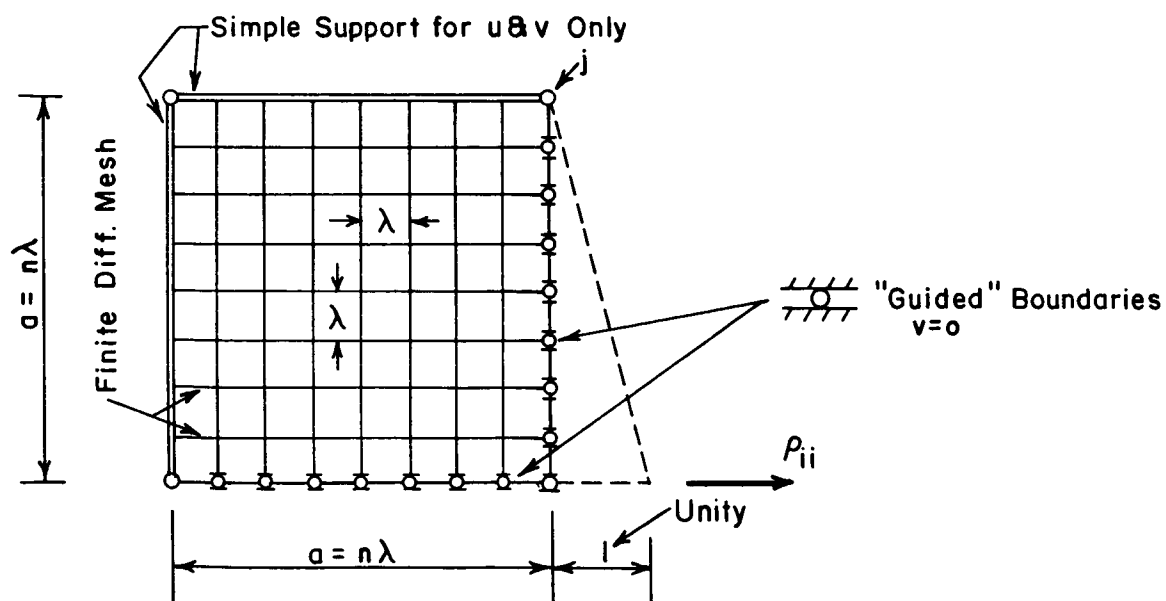Figure 10.   Method of Images for In-Plane Motions

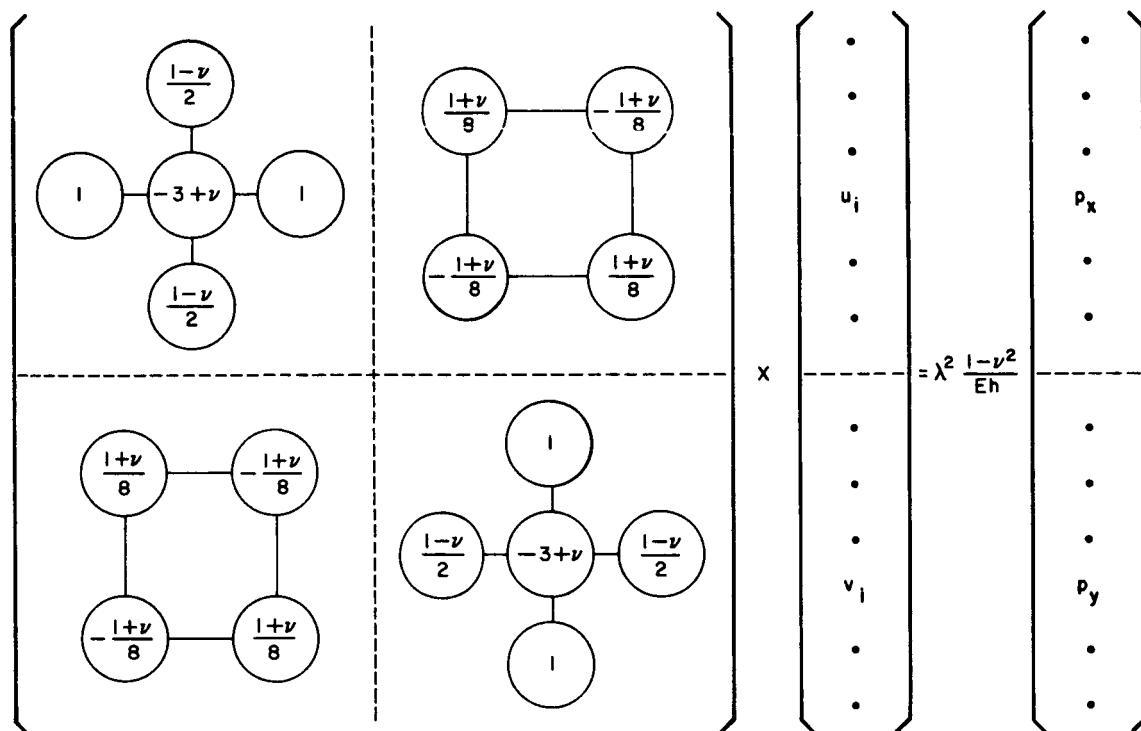Figure 11.   Subdivision for Finite Difference Solution

Figure 12.   Symbolic Arrangement of the Finite Difference Solution (Membrane)

In order to achieve the required symmetry in the stiffness matrix of the element, virtual work of the external forces (active and reactive) has been utilized. The possibility of achieving symmetry in stiffness matrix via change in potentials of external forces instead of the customary internal ones, as far as the author knows, has been overlooked by previous investigators.[29]

Let us assume that the stress field $\{\sigma_i\}$ due to the imposed unit motion of node "i" and due to the linear edge displacement between nodes "i" and "j" as shown in Figure 13a has been already determined. The stress field $\{\sigma_i\}$ is an equilibrium field if we consider all the edge forces. By introducing a small compatible virtual displacement at node "j" while holding the other nodes fixed (Figure 13) we introduce a compatible strain or displacement field $\{\epsilon_j\}$.

Virtual work is a scalar product of two vectors having the same direction, which can be expressed in terms of internal potentials:

$$WK_{virtual} = \int_V \{\sigma_i^T\} \{\epsilon_j\} dV \tag{25}$$

where

$$\{\sigma_i\} = \begin{Bmatrix} \sigma_x \\ \sigma_y \\ \tau \end{Bmatrix} = \frac{E}{1-\nu^2} \begin{bmatrix} 1 & \nu & 0 \\ \nu & 1 & 0 \\ 0 & 0 & \frac{1-\nu}{2} \end{bmatrix} \begin{Bmatrix} \dfrac{\partial u_i}{\partial x} \\[2mm] \dfrac{\partial v_i}{\partial y} \\[2mm] \dfrac{\partial u_i}{\partial y} + \dfrac{\partial v_i}{\partial x} \end{Bmatrix} \tag{26}$$

The strain matrix of the compatible displacement field is:

$$\{\epsilon_j\} = \begin{Bmatrix} \epsilon_x \\ \epsilon_y \\ \gamma \end{Bmatrix} = \begin{Bmatrix} \dfrac{\partial u_j}{\partial x} \\[2mm] \dfrac{\partial v_j}{\partial y} \\[2mm] \dfrac{\partial v_j}{\partial y} + \dfrac{\partial v_j}{\partial x} \end{Bmatrix} \tag{27}$$

The integration shown in equation (25) should be extended over the total volume of the element.

(a)

Stress Field $\left\{F_i\right\}$

(b)

Virtual Displacement Field $\left\{d_j\right\}$
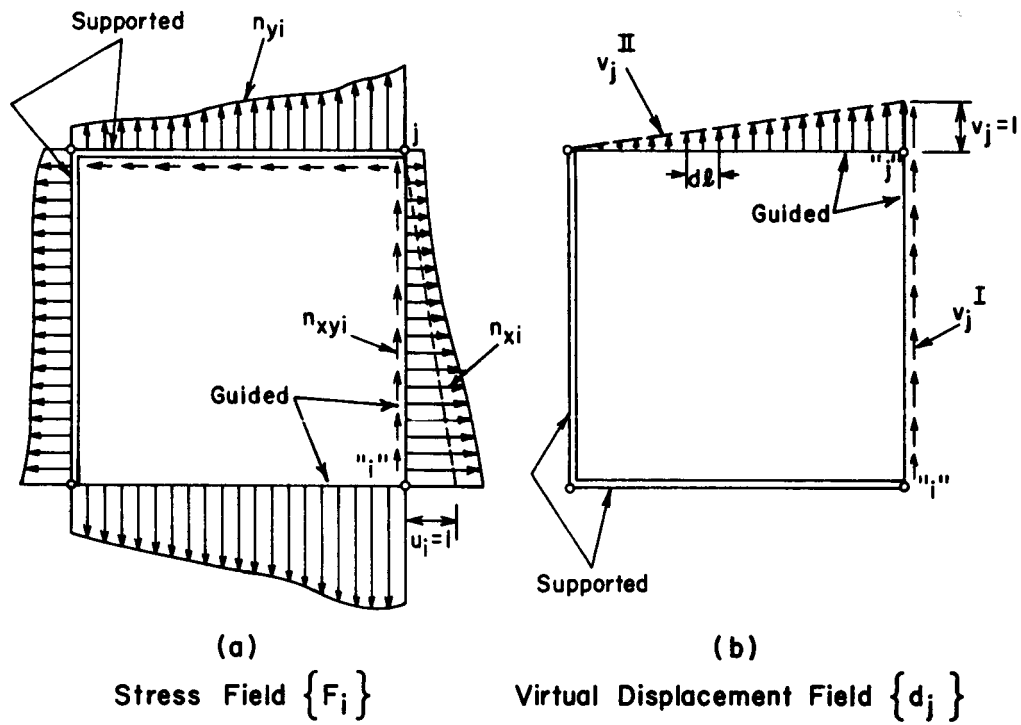
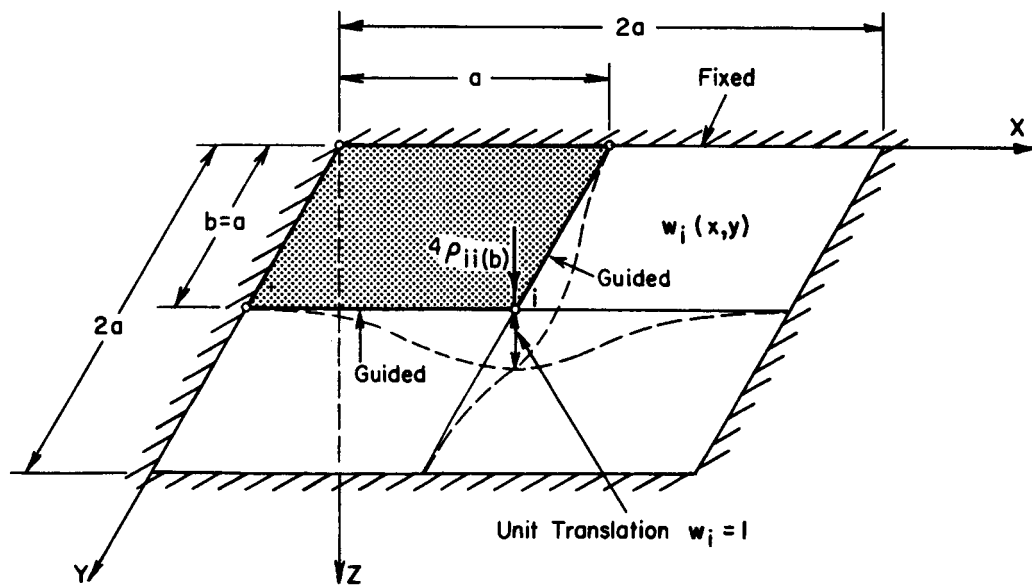Figure 13.   Virtual Work (In-Plane Motions)

Figure 14.   Method of Images for Lateral Translation

The virtual work of the edge forces $\{F_i\}$ and the compatible edge displacement $\{d_j\}$ are obtained from:

$$WK_{virtual} = \oint_{\ell} \{F_i^T\} \{d_j\} \, d\ell, \tag{28}$$

where the matrices of distributed edge forces and edge displacements are:

$$\{F_i\} = \left\{ \begin{array}{c} n_{xi} \\ n_{yi} \\ n_{xyi} \end{array} \right\} \text{ and } \{d_j\} = \left\{ \begin{array}{c} u_j \\ v_j \\ \theta_j \end{array} \right\} . \tag{29}$$

The integration indicated in equation (28) must be extended to all edges of the discrete element.

Since the virtual work of the edge forces must be equal to that of the internal forces, we may write:

$$\int_V \{\sigma^T\} \{\epsilon_j\} \, dV = \oint_{\ell} \{F_i^T\} \{d_j\} \, d\ell . \tag{30}$$

The virtual work of the concentrated force and moment at the node points must equal the virtual work of the internal forces, consequently

$$\rho_{ij} \, 1 = \int_V \{\sigma^T\} \{\epsilon_j\} \, dV , \tag{31}$$

from which utilizing equation (30) the required stiffness coefficients can be obtained:

$$\rho_{ij} = \oint_{\ell} \{F_i^T\} \{d_j\} \, d\ell , \tag{32}$$

but since

$$\rho_{ji} = \int_V \{\sigma_j^T\} \{\epsilon_i\} \, dV = \int_V \{\sigma_i^T\} \{\epsilon_j\} \, dV = \rho_{ij} , \tag{33}$$

the required symmetry of the stiffness matrix of the element has been established.

The results of these computations, expressed in the local coordinate system are given for a square discrete element in Table I. The sign convention and the numbering system of the motions and forces are shown in Figure 4.

Eight free body motions of the corner nodes have been considered. The rotation around the Z axis, due to the rigidity of the shell to resist such motion has been neglected. The first subscript indicates the location and direction of the force, while the second refers to the motion which has caused it.

A lengthy computation, such as described above, always requires intermediate checks in order to avoid repeated errors. The first check applied was satisfaction of equilibrium of the active and reactive forces in form of:

$$\Sigma X = 0, \quad \Sigma Y = 0, \quad \Sigma M_z = 0 \ . \tag{34}$$

The second check should consist of the pointwise satisfaction of Maxwell's law of reciprocity

$$\{F_{ij}\} = \{F_{ji}\} \ . \tag{35}$$

The symmetry of the stiffness matrix[13] represents the third check. While the fourth check is again an equilibrium check[14] of the concentrated forces assigned to the node points. That is to say, the columns of the stiffness matrix must satisfy the macroscopic equilibrium condition discussed previously. The final and most important check is the testing of the convergence characteristics of the discrete element solution against known analytical solutions as is discussed in Section XI of this report.

Finally it should be mentioned that obtaining stiffness matrices by the above mentioned procedure is tedious, but computers can ease the burden of the task considerably. Since the numbers are reusable, they should be computed only once for any geometry or aspect ratio.

Table I. Membrane Part of the Stiffness Coefficients[*]

$$[\rho_{ij(m)}] = $$

	1	2	3	4	5	6	7	8
1	0.429							
2	0.1674	0.429						
3	-0.254	0.0073	0.429		SYMMETRIC			
4	-0.0073	0.079	-0.1674	0.429				
5	-0.254	-0.1674	0.079	0.0073	0.429			
6	-0.1674	-0.254	-0.0073	-0.254	0.1674	0.429		
7	0.079	-0.0073	-0.254	0.1674	-0.254	0.0073	0.429	
8	0.0073	-0.254	0.1674	-0.254	-0.0073	0.079	-0.1674	0.429

$$\times \quad \frac{Eh}{1-\nu^2}$$

Note: For numbering and sign convention, see Figure 4.

VII. DERIVATION OF THE FLEXURAL PART OF THE STIFFNESS COEFFICIENTS

The procedure to obtain the stiffness coefficients due to bending of the flat discrete elements is essentially the same as described in the preceeding section for in-plane motions. The small element deformation patterns due to unit nodal displacements are affine to (but not the same as) those of a beam subjected to bending, which can be described by cubic type polynominal expressions.

In order to avoid any "guessing" concerning the form of the deflection patterns unit motions (lateral translation and compatible rotations) are introduced at the node points. Applying again the method of images (Figure 14) the edge reactions due to these motions are obtained by solving the differential equation of the plate problem[22] and the resulting edge forces[14] by a finite difference method (Figures 15 and 16) using 10 X 10 subdivision.

The differential equation of a plate in finite difference form can be expressed as

$$20w_0 - 8(w_1 + w_2 + w_3 + w_4) + 2(w_5 + w_6 + w_7 + w_8) +$$
$$+ w_9 + w_{10} + w_{11} + w_{12} = \frac{\lambda^2 (P_z = 1)}{D} \quad . \tag{36}$$

Unit translation at node point "i" is obtained by a simple normalization process

$$\frac{P_z = 1}{w_i} = \frac{P_z^*}{w_i^* = 1} \quad . \tag{37}$$

In order to check the accuracy of the finite difference solution the deflection surface $w_i(x, y)$ has been computed using Galerkin's method. The deflected plate surface has been approximated by the following double Fourier series:

$$w_i(x, y) = \frac{1}{4} \sum_m \sum_n W_{mn} \left(1 - \cos \frac{m \pi x}{a} \right) \cdot \left(1 - \cos \frac{n \pi y}{a} \right) \quad .$$

$$m = 1, 3, 5 \ldots \qquad n = 1, 3, 5 \ldots \tag{38}$$

Figure 15. Finite Difference Solution for Plate Bending

Figure 16. Finite Difference Grid Reference

A concentrated load in magnitude of $4P_z = 4$ has been applied at the center ($x = a$, $y = a$) of the image plate of magnitude $2a \times 2a$ size, and the result has been normalized according to equation (37). A good agreement between the analytical and finite difference solutions has been established.

The compatible unit rotation of the plate has been obtained by prescribing the pertinent beam deflections at the edge of the plate and solving equation (36) for the prescribed edge displacements.

The distributed forces and moments along the edges of the discrete element have been computed using finite difference forms[7] of equation (14). The assignment of the distributed edge forces to the corner node points has followed the previously described method based on virtual work on the edge forces as given by equation (32). Displacement patterns to one specific application of virtual work concept are shown in Figure 18. The bending part of the stiffness matrix of a rectangular discrete element is given in Table II.

The macroscopic equilibrium of the element in form of

$$\Sigma M_x \cong 0; \quad \Sigma M_y \cong 0; \quad \Sigma Z \cong 0 \tag{39}$$

has been again approximately satisfied.

In dealing with arbitrary geometrical shapes the use of trapezoidal discrete element is mandatory. Trapezoidal discrete elements, can be approximated as shown in Figure 19.

If the original structure is a plate, compatibility requirements of stresses and displacements within the element and at the edges of the adjoining element has been completely satisfied. In case of shells, however, compatibility of slopes at the edges is violated since curved surfaces are approximated by flat elements. The violation of slope compatibility can be removed only by introduction of curved elements.[24]

Finally, in connection with development of the bending part of the stiffness coefficients, the large element behavior of discrete shell elements should be mentioned. As has been discussed earlier the small element behavior of a plate in bending resembles that of a beam, while its large element behavior resembles that of a beam on elastic foundation as shown in Figure 20. The convergence of the derived solution is described in Section XI.
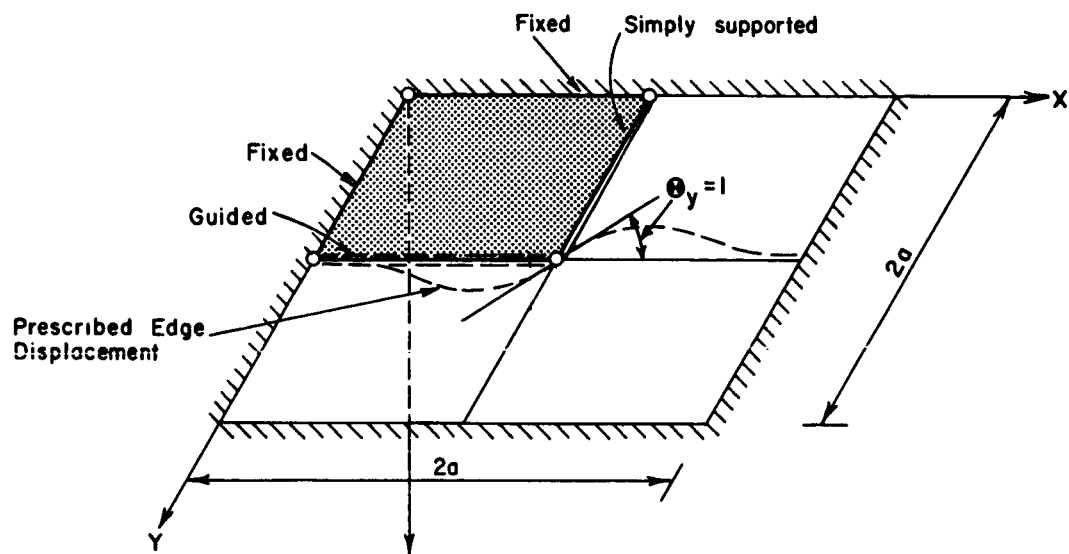
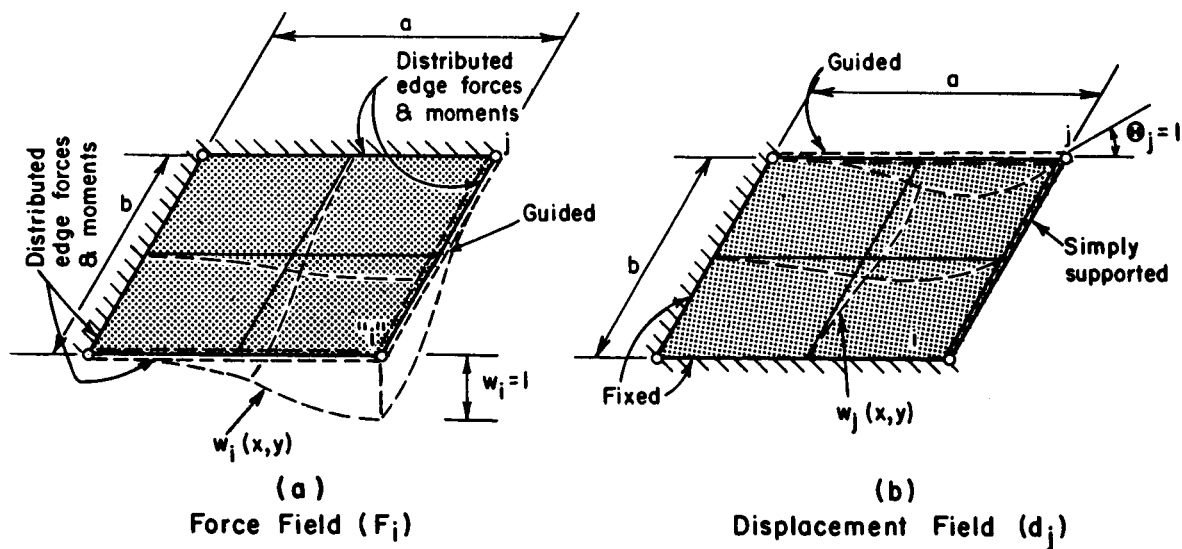Figure 17.   Unit Rotation of a Node Point

(a)
Force Field (F$_i$)

(b)
Displacement Field (d$_j$)

Figure 18.   Virtual Work (Bending)

Table II. Bending Part of the Stiffness Coefficients*

$$[\rho_{ij(b)}] = \frac{Eh^3}{12(1-\nu^2)} \times$$

	9	10	11	12	13	14	15	16	17	18	19	20
9	$\frac{11.083}{a^2}$											
10	$\frac{3.248}{a}$	1.8038							SYMMETRIC			
11	$-\frac{3.248}{a}$	-0.94808	1.8038									
12	$\frac{5.4463}{a^2}$	$-\frac{1.9711}{a}$	$\frac{0.42965}{a}$	$\frac{11.083}{a^2}$								
13	$\frac{1.9711}{a}$	0.54247	-0.16786	$-\frac{3.248}{a}$	1.8038							
14	$\frac{0.42965}{a^2}$	0.16786	0.0752	$-\frac{3.248}{a}$	0.94808	1.8038						
15	$-\frac{0.19326}{a^2}$	$\frac{0.84867}{a}$	$\frac{0.84867}{a}$	$\frac{5.4463}{a^2}$	$\frac{0.42965}{a}$	$\frac{1.9711}{a}$	$\frac{11.083}{a^2}$					
16	$\frac{0.84867}{a}$	$\frac{0.39747}{a}$	-0.3305	$\frac{0.42965}{a}$	0.0752	-0.16786	$-\frac{3.248}{a}$	1.8038				
17	$-\frac{0.84867}{a}$	-0.33035	0.39747	$\frac{1.9711}{a}$	0.16786	0.54247	$\frac{3.248}{a}$	-0.94808	1.8038			
18	$\frac{5.4463}{a^2}$	$\frac{0.42965}{a}$	$\frac{1.9711}{a}$	$\frac{0.19326}{a^2}$	$\frac{0.84867}{a}$	$\frac{0.84867}{a}$	$\frac{5.4463}{a^2}$	$\frac{1.9711}{a}$	$\frac{0.42965}{a}$	$\frac{11.083}{a^2}$		
19	$\frac{0.42965}{a}$	0.0752	0.16786	$\frac{0.84867}{a}$	0.39747	0.33035	$-\frac{1.9711}{a}$	0.54247	-0.16786	$\frac{3.248}{a}$	1.8038	
20	$-\frac{1.9711}{a}$	$-\frac{0.16786}{a}$	$\frac{0.54247}{a}$	$-\frac{0.84867}{a}$	0.33035	0.39747	$-\frac{0.42965}{a}$	0.16786	0.0752	$\frac{3.248}{a}$	0.94808	1.8038

* For numbering and sign convention, see Figure 4.
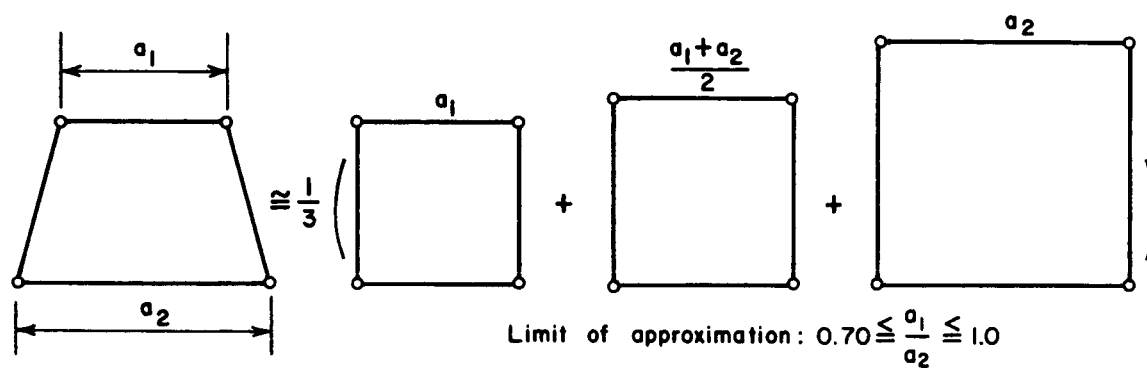 b = a for square element

37

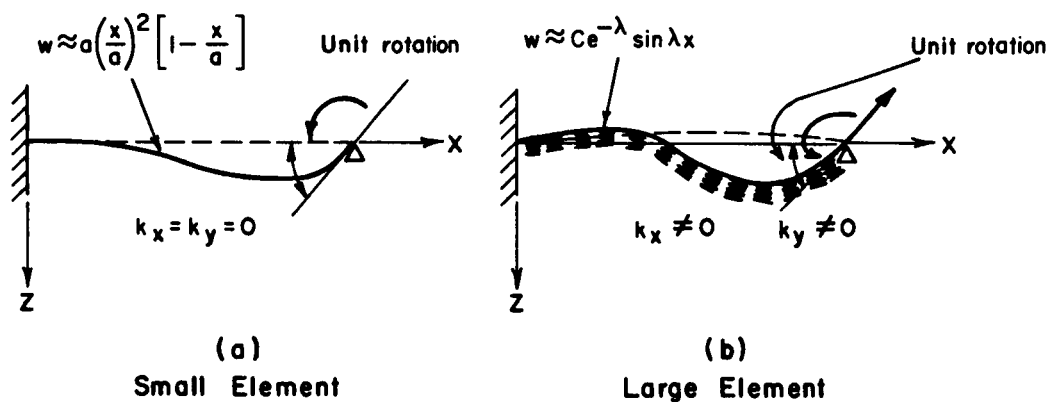Figure 19. Approximation of Trapezoidal Discrete Elements

Figure 20. Small vs. Large Element Behaviors of Shells Subjected to Bending

VIII.   ARBITRARY DYNAMIC LOADS AND INERTIA FORCES

In most cases the stress analyst is confronted with the deter-
mination of the dynamic response of shells of arbitrary shape subjected
to arbitrary (in space and time) dynamic loadings.   Because of the com-
plexity of the problem either "equivalent" static loading or other type
of crude approximations are used.

The matrix method described herein permits the consideration
of any arbitrary loads, (including blast loads) regardless of its space
and time variation.   Let us discuss first the time dependency of such
a load.

Equation (12) can be written in the following form:

$$\{P_i(t)\} = \sum_m \{R_i^T\} \left\{ \mathcal{R}_{im} \right\} \sin p_m t , \tag{40}$$

where $\{\mathcal{R}\}_{im} \sin p_m t$ represents the time dependent part of the dynamic
force, and

$$P_m = \frac{m\pi}{T} \tag{41}$$

is the circular frequency of the Fourier expansion while $\{R_i\}$ is the
column vector of the generalized nodal forces.

Any arbitrary time variation can be expressed by Fourier sine
series, since by proper continuation of the forcing function even a non-
periodic load can be made periodic.   In Figure 21 a blast load is shown.
Using $T = (10 \rightarrow 15)t_0$ for the half period of expansion the effect of the
fictitious negative load can be retarded long enough so that it does not
influence the dynamic response of the structure to the real load.   The
validity of this statement will be proven by numerical example in
Section XI.

Following the rules of Fourier Series expansion of an arbitrary
function f(t) the amplitudes of the time dependent part are obtained
from:

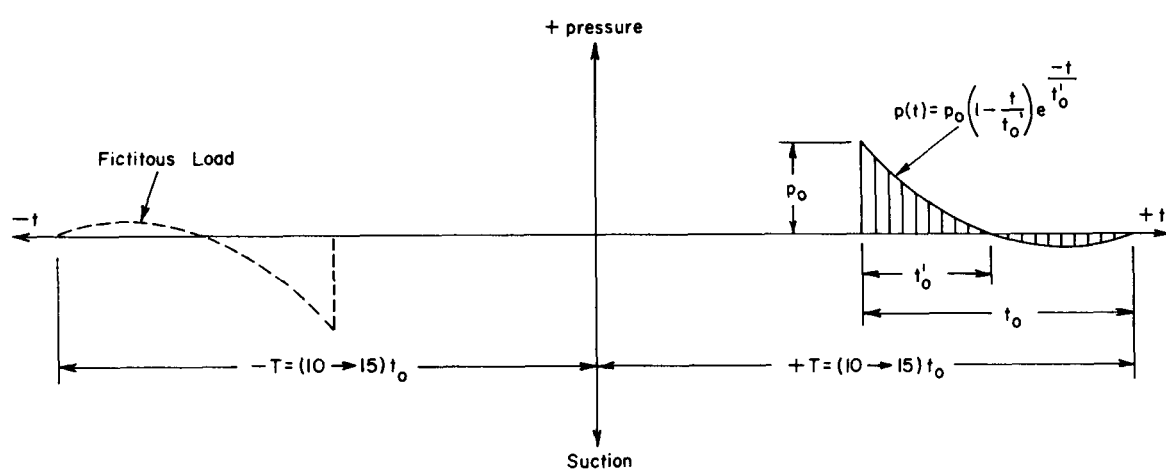$$\mathcal{R}_{im} = \frac{2}{T} \int_0^T f(t) \sin \frac{m\pi}{T} dt . \tag{42}$$

Figure 21. Fourier Approximation of a Blast Load

If the forcing function f(t) can not be expressed analytically or the evaluation of the integral in equation (42) is too time consuming numerical integrals can be used to advantage.

The simplest way to handle loads which are distributed arbitrarily in space is to assign concentrated forces and moments to the node points which are <u>statically equivalent</u> (force and moment) to the arbitrary distributed loads acting on $\dfrac{a \times b}{4}$ surface of one element. This approximation yields satisfactory results only if relatively large numbers of elements are used.

If the subdivision is coarse, or a "large element" approach is used, the proper representation of variable surface loads by generalized nodal forces are of increased importance. It can be stated that the accuracy of the discrete element solution of dynamic shell problems is markedly improved by proper load representation, which includes the inertia forces.

The components of the nodal forces in the local coordinate system, (see equation (40)) which are equivalent to arbitrary distributed loads acting on a discrete shell element is obtained from virtual work:

$$R_j = \int_0^a \int_0^b \{\delta_j(x, y)\}_{virtual}^T \cdot \{p(x, y)\}\, dx dy, \tag{43}$$

which in case of lateral loading takes the form of:

$$R_{zj} = \int_0^a \int_0^b w_j(x, y)_{virtual} \cdot p_z(x, y)\, dx dy, \tag{43a}$$

where $w_j(x, y)$ is obtained from the virtual unit displacement of node "j" in the Z direction, while the other nodes are held fixed. Since the resulting deflected surfaces considering small element behavior, have been already obtained for determination of stiffness coefficients, the numerical evaluation of the double integral by computer is quickly achieved. In Table III u(x, y) and v(x, y) values for unit in-plane motion are listed, while Tables IV and V give the numerical values of w(x, y) for unit translation and for compatible unit rotation of the nodes, respectively.

Since equation (43) is not as sensitive to approximation of deflected surfaces, as the determination of stiffness coefficients is, usable values can be obtained for the generalized nodal forces by approximating the above mentioned three displacement components by:

Table III. Displacement Components in X and Y Direction (u, v) Obtained from Straight Line Edge Motion

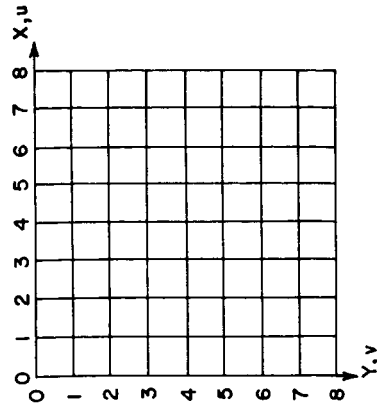| y	x	1	2	3	4	5	6	7	8
1	u	0.0108	0.0189	0.0278	0.0387	0.0525	0.0699	0.0923	0.1250
	v	0.0130	0.0229	0.0307	0.0363	0.0385	0.0355	0.0243	0.0000
2	u	0.0168	0.0327	0.0512	0.0746	0.1044	0.1423	0.1899	0.2500
	v	0.0187	0.0347	0.0474	0.0561	0.0588	0.0528	0.0344	0.0000
3	u	0.0203	0.0430	0.0711	0.1073	0.1541	0.2137	0.2875	0.3750
	v	0.0206	0.0391	0.0542	0.0645	0.0677	0.0606	0.0391	0.0000
4	u	0.0225	0.0507	0.0874	0.1359	0.1994	0.2811	0.3822	0.5000
	v	0.0199	0.0383	0.0538	0.0649	0.0690	0.0627	0.0413	0.0000
5	u	0.0236	0.0560	0.0999	0.1590	0.2377	0.3409	0.4712	0.6250
	v	0.0171	0.0334	0.0476	0.0585	0.0638	0.0601	0.0414	0.0000
6	u	0.0241	0.0593	0.1084	0.1754	0.2665	0.3892	0.5505	0.7500
	v	0.0126	0.0249	0.0362	0.0455	0.0516	0.0517	0.0390	0.0000
7	u	0.0241	0.0609	0.1129	0.1848	0.2837	0.4208	0.6127	0.8750
	v	0.0068	0.0135	0.0198	0.0257	0.0306	0.0337	0.0305	0.0000
8	u	0.0241	0.0613	0.1143	0.1877	0.2893	0.4321	0.6427	1.0000
	v	0.0000	0.0000	0.0000	0.0000	0.0000	0.0000	0.0000	0.0000

Table IV. Lateral Displacement Components w(x, y) Obtained from Unit Translation of the Node Point in Z Direction.

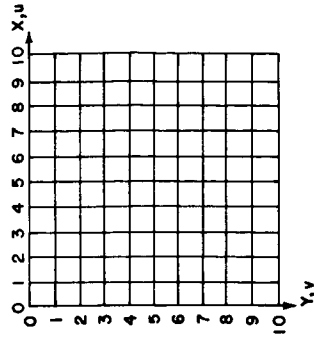| y \ x	0	1	2	3	4	5	6	7	8	9	1C
0	0.0000										
1	0.0000	0.0002									
2	0.0000	0.0017	0.0076				SYMMETRIC				
3	0.0000	0.0044	0.0176	0.0384							
4	0.0000	0.0080	0.0304	0.0645	0.1065						
5	0.0000	0.0120	0.0448	0.0933	0.1528	0.2182					
6	0.0000	0.0161	0.0591	0.1223	0.1994	0.2842	0.3705				
7	0.0000	0.0198	0.0722	0.1488	0.2420	0.3452	0.4511	0.5518			
8	0.0000	0.0228	0.0828	0.1700	0.2765	0.3949	0.5180	0.6373	0.7419		
9	0.0000	0.0247	0.0896	0.1839	0.2991	0.4278	0.5628	0.6961	0.8171	0.9100	
10	0.0000	0.0254	0.0919	0.1887	0.3069	0.4393	0.5787	0.7173	0.8454	0.9486	1.0000

Table V. Lateral Displacement Components w(x, y) Obtained from Unit Rotation of Node Point Around Y Axis.

x\y	0	1	2	3	4	5	6	7	8	9	10
0	0.0000	0.0000	0.0000	0.0000	0.0000	0.0000	0.0000	0.0000	0.0000	0.0000	0.0000
1	0.0000	0.0003	0.0009	0.0018	0.0027	0.0035	0.0040	0.0041	0.0036	0.0023	0.0000
2	0.0000	0.0009	0.0033	0.0066	0.0100	0.0130	0.0150	0.0153	0.0133	0.0084	0.0000
3	0.0000	0.0019	0.0069	0.0136	0.0207	0.0270	0.0311	0.0318	0.0276	0.0175	0.0000
4	0.0000	0.0032	0.0113	0.0222	0.0338	0.0440	0.0507	0.0517	0.0451	0.0285	0.0000
5	0.0000	0.0045	0.0160	0.0315	0.0480	0.0625	0.0720	0.0735	0.0640	0.0405	0.0000
6	0.0000	0.0058	0.0207	0.0408	0.0622	0.0810	0.0933	0.0953	0.0829	0.0525	0.0000
7	0.0000	0.0071	0.0251	0.0494	0.0753	0.0980	0.1129	0.1152	0.1004	0.0635	0.0000
8	0.0000	0.0080	0.0287	0.0564	0.0860	0.1120	0.1290	0.1317	0.1147	0.0726	0.0000
9	0.0000	0.0875	0.0311	0.0612	0.0933	0.1215	0.1400	0.1429	0.1244	0.0787	0.0000
10	0.0000	0.0900	0.0320	0.0630	0.0960	0.1250	0.1440	0.1470	0.1280	0.0810	0.0000
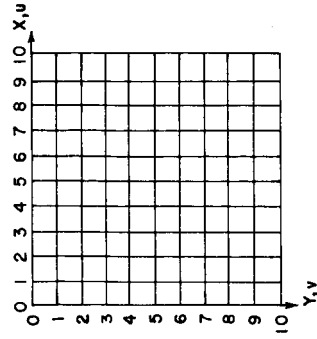
$$u_i(x, y) = \frac{x}{a}\frac{y}{b} \tag{44}$$

$$v_i(x, y) = 0,$$

and

$$w_i^I(x, y) = \left[3\left(\frac{x}{a}\right)^2 - 2\left(\frac{x}{a}\right)^3\right] \cdot \left[3\left(\frac{y}{b}\right)^2 - 2\left(\frac{y}{b}\right)^3\right], \tag{45}$$

or

$$w_i^{II}(x, y) = \left[a\left(\frac{x}{a}\right)^2\left(1 - \frac{x}{a}\right)\right] \cdot \left[3\left(\frac{y}{b}\right)^2 - 2\left(\frac{y}{b}\right)^3\right]. \tag{46}$$

The previously described rotation of coordinate system will express the force components in the general reference coordinate system.

A similar procedure can be followed in case of inertia forces substituting

$$p(x, y) = \overline{m}\ \ddot{\delta}_{virtual}, \tag{47}$$

into equation (43), where $\overline{m}$ represents the mass of the element per unit area and the two dots are the second derivatives with respect to time, representing the acceleration of the structure.

Especially in case of free vibrations the use of "consistent mass" matrix, whose elements are derived from the kinetic energy associated with the displacement of the shell elements, is of basic importance.

The coefficient $\mathcal{M}^0{}_{ij}$ of $\left[\ \mathfrak{M}^0{}_{ij}\right]$ matrix (in local coordinate system) are obtained from[17,30]

$$\mathcal{M}^0{}_{ij} = \int_0^a\int_0^b \overline{m}\ \Phi_i(x, y)\ \Phi_j(x, y)\,dxdy, \tag{48}$$

where Φ_i and Φ_j are displacement functions associated with the unit point displacement $\delta_i = 1$ and $\delta_j = 1$, respectively, when all other nodes of the element are fixed.

Since $\Phi_i(x, y)$ and $\Phi_j(x, y)$ are the very same displacement components required for the determination of elements of the stiffness matrix, their values can be obtained either from Tables III, IV and V or from equations (44), (45) and (46).

Again a rotation of the coordinate system similar to that used in case of stiffness coefficients will transform the consistent mass matrix from the local to the intermediate or general reference coordinate systems:

$$\left[\mathcal{M}_{ij} \right] = \left[\diagdown_{T} \right]^{-1} \left[\mathcal{M}^{0}_{ij} \right] \left[\diagdown_{T} \right] . \tag{49}$$

IX.   AUTOMATION OF THE COMPUTATION

The elements k_{ij} of the stiffness matrix expressed in the general reference coordinate system can be easily compiled into the stiffness matrix $[k_{ij}]$ of the entire structure without resorting to tedious element by element input approach.   First $[k_{ij}]$ matrix expressed in intermediate coordinate system is altered to take care of the boundary conditions as described previously.   Then a proper numbering system is introduced, which would result in a band matrix, heavily populated in the vicinity of the main diagonal.   This can be achieved by: (1) proper grouping of nodal points, and (2) using proper sequential order in numbering the displacements at each node point.

No set rules can be given for grouping of node points since it depends largely on the geometry of the total structure.   In case of long cylindrical shells, for instance, meridional grouping is more expedient than longitudinal; while longitudinal grouping might be superior for short cylindrical shells.

Within each group the u, v, w, θ_x, θ_y, displacements are collected point wise following a predetermined sequence (u, v, w, θ_x, θ_y). This procedure yields five band matrices containing fully populated submatrices.

A descriptive flow diagram for automatic compiling the stiffness matrix is shown in Figure 22.   The same flow chart can be applied logically for compilation of the "consistent" mass matrix $\left[\mathfrak{M}_{ij} \right]$. Figures 23 and 24 show the flow chart of computer solutions for forced and free vibration analyses respectively.

Eigenvalue, eigenvector and matrix inversion computer routines for large matrices have been checked and documented by Denver Research Institute under a NASA Research Grant.[31]

START ——→ Initialize all Array
Locations R(I, J) = 0

Index = 1

(H) Read Elem (L, M)

Where L is Index No. and M
Indicates Sub-structure

Are All Elements Read
and Placed in Matrix?

Go to (F) ←— Yes

No

Go to A, B, or C depending
on value of M

(A) *Sub-routine for Compiling
Matrix for Sub-structure $i_1 - i_8$
(Engine cluster)
$I = I_a, I_b, I_c \cdots$
$J = J_d, J_e, J_f \cdots$

$J_i \geq I_i$
Go to G

(B) *Sub-routine for Compiling
Matrix for Sub-structures
$i_9, i_{10}, i_{11} \cdots$
Go to G   (Fins)

(C) *Sub-routine for Compiling
Matrix for Sub-structures
$i_p, i_q, i_r \cdots$
(Boundary points)
Go to G

.
.
.
etc.

(G) Index = Index + 1
Go to Read (H)

(F) All Elements of Upper Triangular Array
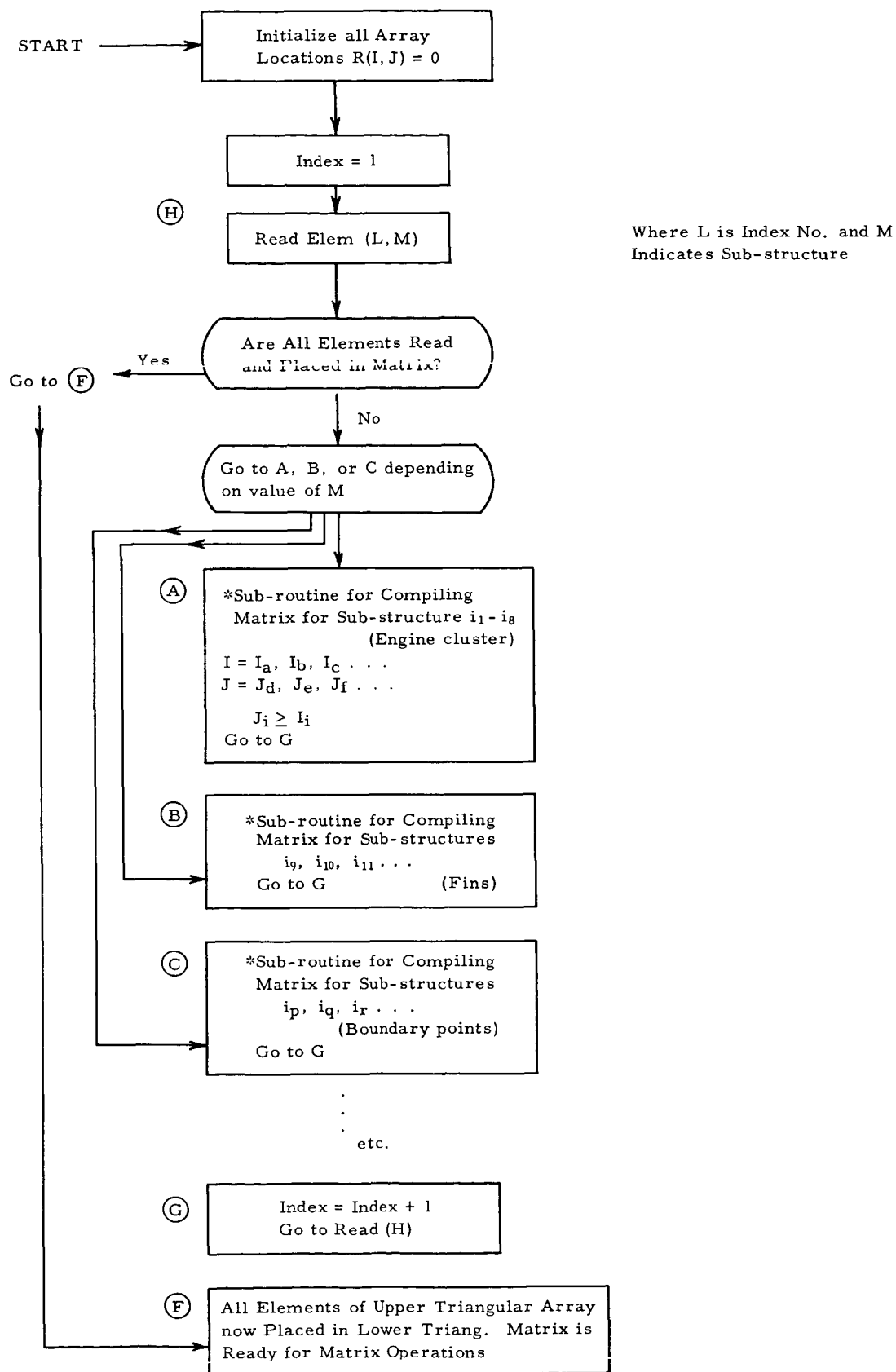now Placed in Lower Triang. Matrix is
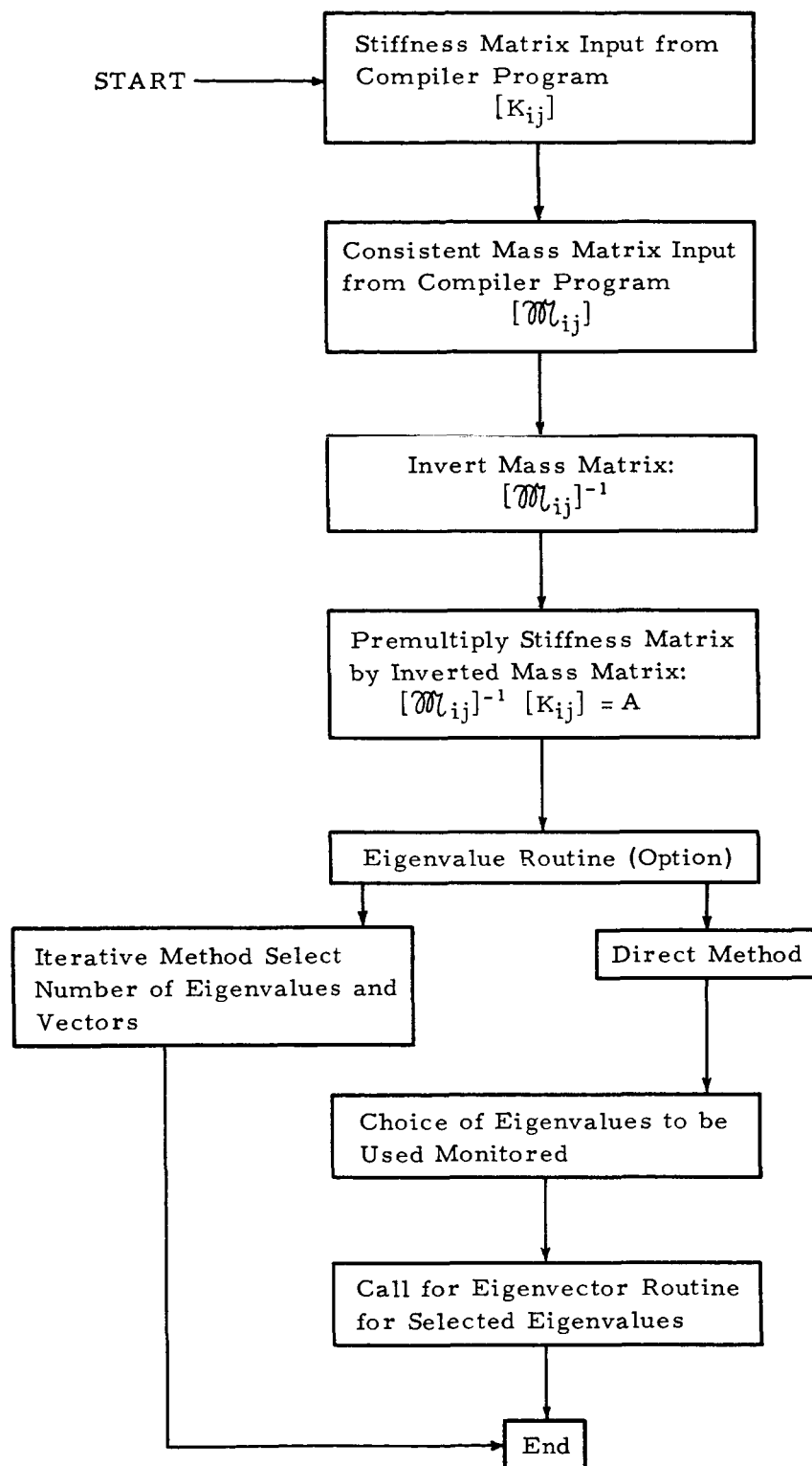Ready for Matrix Operations

Figure 22. Flow Chart for Compilation of Stiffness Matrix

Figure 23. Flow Chart for Free Vibration Computation

Figure 24.   Flow Chart for Forced Vibration Computation
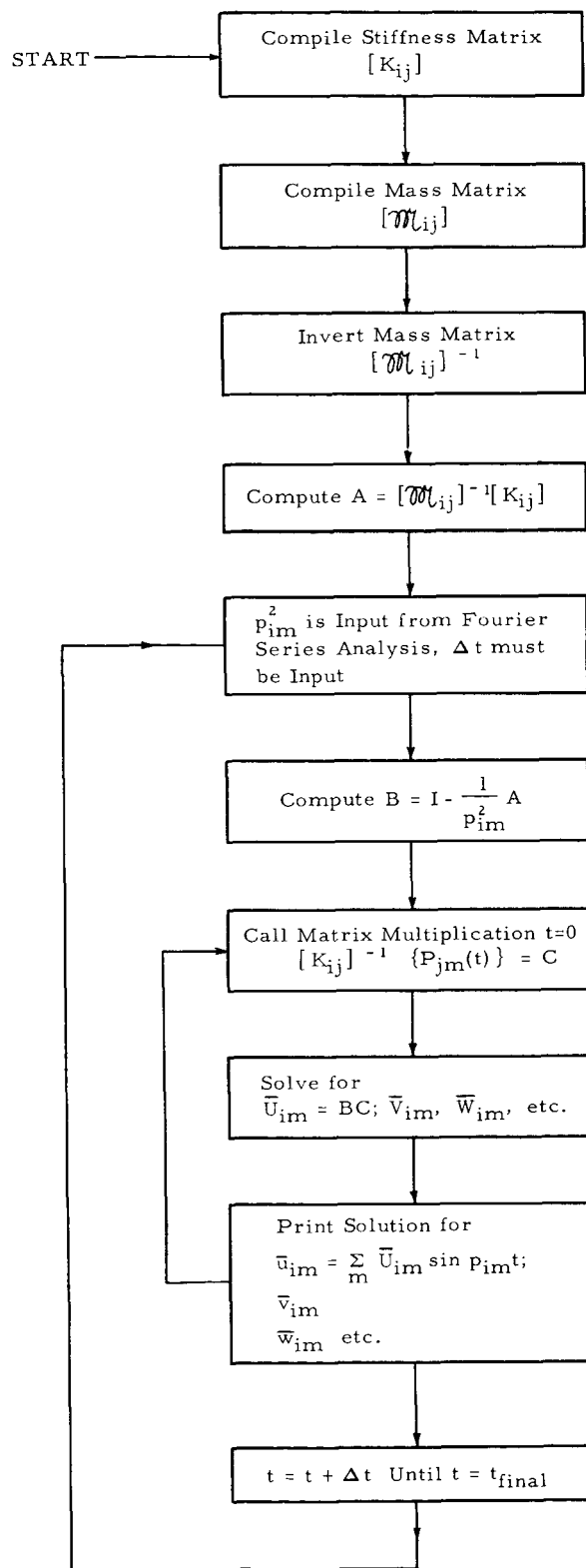
The flowchart contains the following boxes:

START →

Compile Stiffness Matrix
$[K_{ij}]$

Compile Mass Matrix
$[\mathcal{M}_{ij}]$

Invert Mass Matrix
$[\mathcal{M}_{ij}]^{-1}$

Compute A = $[\mathcal{M}_{ij}]^{-1}[K_{ij}]$

p_{im}^2 is Input from Fourier Series Analysis, Δt must be Input

Compute B = I - $\frac{1}{p_{im}^2}$ A

Call Matrix Multiplication t=0
$[K_{ij}]^{-1}$ $\{P_{jm}(t)\}$ = C

Solve for
$\overline{U}_{im}$ = BC; $\overline{V}_{im}$, $\overline{W}_{im}$, etc.

Print Solution for
$\overline{u}_{im} = \sum_m \overline{U}_{im} \sin p_{im}t;$
$\overline{v}_{im}$
$\overline{w}_{im}$ etc.

t = t + Δt Until t = t_{final}

X.   MATHEMATICAL PROBLEMS INHERENT TO LARGE MATRICES

The algebraic manipulation of matrices and matrix equations presents no problem for solution of all the elementary operations as well as for the characteristic numbers or eigenvalues. The methods are numerous and well expounded in the literature and computer programs are plentiful. [31]

Reduction techniques, elimination methods, triangular factoring, diagonalization, and all the refinements of these methods for finding a matrix inverse are subject to large errors because of simple round-off. Two methods customarily used to reduce this error are column scaling (not suitable for all matrices) and the use of double-precision computer arithmetic, which more than doubles the significant digits of each number but necessitates the use of subroutines which increase computation time on the order of two to three times, a prohibitively high price for most applications. In addition, valuable machine storage is lost. The direct methods (non-iterative) of matrix inversion are generally recognized to be well suited to computer techniques because they permit the reduction of a matrix, A, to an array which can be saved for use at any time of solution of the matrix equation, $[A] \{X\} = \{B\}$ with different righthand sides. In order to avoid slow iterative refinements, there is a real need for error analysis and the choice of computational methods which minimize the errors that are intrinsic to the computations in solving the problem of the general matrix of large order. The alternative Monte Carlo methods provide a simple computational approach to the statistical estimation of the elements of the inverse which are not affected substantially by round-off and truncation error, but the statistical variation of the results tends to be quite large in most cases until refined by many additional random walks. Therefore, the technique is most widely used for obtaining rough estimates very quickly, and for single column inversions, useful for point loads. An iterative process for improving the inverted matrix to be computed to as high a degree of accuracy as is required, but for very large matrices computer time for handling the necessary matrix subtractions and multiplications may be extremely costly. Partitioning techniques are widely used for large matrices. For a non-definite and sparse matrix the problem of selecting a square submatrix of useful size the determinant of which is non-vanishing may be a problem. In any case, the computer operations are many and long and this is usually used as a last resort.

The problems involved in solving for the eigenvalues of a large matrix and the associated eigenvectors can be extremely expensive for a general matrix of very large order. For a matrix size much greater than 150 × 150 auxiliary equipment must be used for finding all the eigenvalues of the system for a general matrix. The accuracy problem is much the same as for finding the inverse and the machine time for an iterative process makes it feasible to solve for only one or two critical values in this manner.

We find, however, that for certain classes of matrices, the accuracy, machine time, and machine storage problems are considerably reduced. These matrix characteristics are:

1. a real and symmetrical matrix

2. a positive-definite matrix

3. a relatively sparse matrix heavily positioned along the main diagonals.

The symmetry requirement is perhaps the most vital in permitting solutions of larger matrices. The number of computer operations is considerably less with almost all methods. For example, with the triangular factoring technique time is cut considerably by virtue of the fact that the upper triangular matrix is also the transpose of the lower. This fact coupled with a theorem which states that the transpose of the inverted unit triangular matrix is equal to the inverse of the transpose permits rapid calculation of the inverse matrix. If a matrix is real and symmetric, we can be assured of real eigenvalues and of a corresponding set of vectors which are orthogonal. Normalization of the vectors provides an orthonormal set of basis vectors in Euclidean n-space, an important fact in eliminating the need for brute force simultaneous equation approach used for locating the vectors of the general set of homogeneous equation. The other requirements stated guarantee the success for a variety of matrix methods, reduce the number of calculations and generally improve accuracy.

The matrices resulting from the analysis described in the foregoing sections are characterized by all of the above, and are solved more quickly and more accurately because of this. Matrix iteration and partitioning may be necessary, but the number of iterations will be reduced and the problem of selecting a leading sub-matrix which is non-vanishing for matrix partitioning is no longer of consequence.

XI.   NUMERICAL EXAMPLES

In order to illustrate the applicability and obtain information concerning the accuracy of the matrix solution of shells, described herein, numerical examples have been worked out and compared with known theoretical solutions.

First the validity of Fourier series representation of suddenly applied blast load has been checked using a one degree of freedom mass-spring system as shown in Figure 25. The arbitrary continuation of the time-load function

$$f(t) = p_0 \left(1 - \frac{t}{t_0}\right) \tag{50}$$

is shown in Figure 25c. Having only sine terms, the Fourier coefficient was computed from (42):

$$b_n = \frac{2}{7t_0} \int_0^{7t_0} f(t) \sin \frac{n\pi}{7t_0} t \, dt = \frac{2p_0}{n\pi} \left(\cos \frac{6}{7} n\pi + \frac{7}{n\pi} \sin \frac{6}{7} n\pi\right). \tag{51}$$

The first eight coefficients of the Fourier series expansion are tabulated in Table VI.

Thus the Fourier (sine) series expansion of the forcing function has the form

$$f(t) = \sum_n b_n \, \sin nt = p_0 \, [0.045 \sin t -$$

$$-0.079 \sin 2t + 0.105 \sin 3t -$$

$$-0.124 \sin 4t + 0.151 \sin 5t - 0.113 \sin 6t + \tag{52}$$

$$+0.091 \sin 7t - 0.063 \sin 8t].$$

Expressing the deflections in a trigonometric series similar to the forcing function

$$x = \sum_n X_n \, \sin nt \tag{53}$$
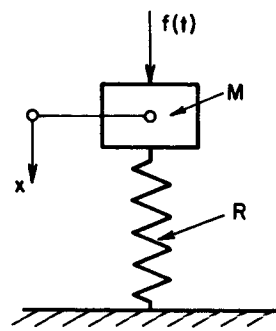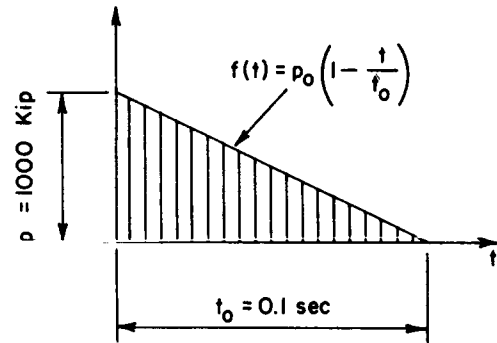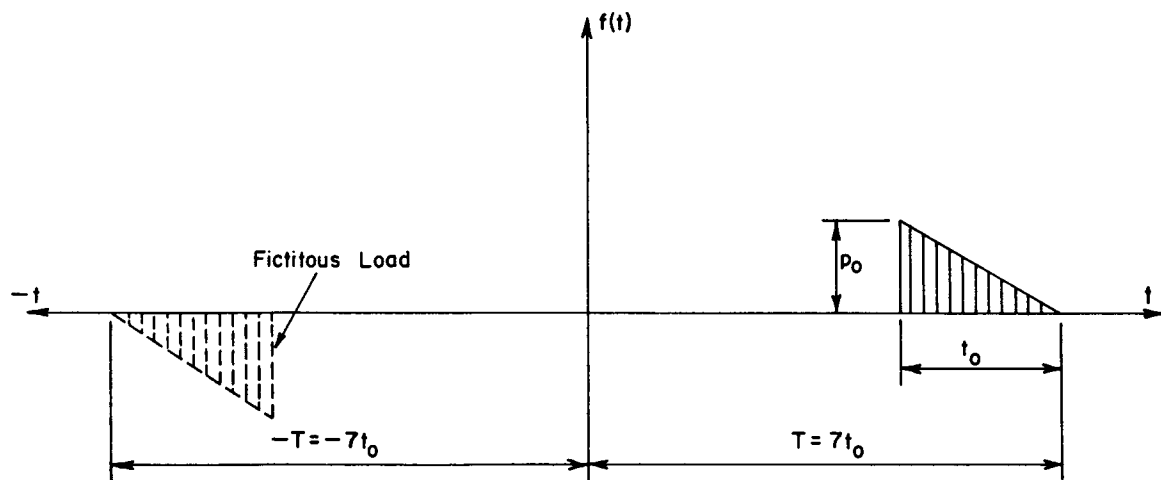
M = 2.5 $\frac{Kip\ sec^2}{ft}$

R = 750 Kip/ft

(a)
Spring – Mass System

(b)
Suddenly Applied Load

(c)
Arbitrary Continuation of Load

Figure 25. Fourier Series Solution of Suddenly Applied Load on One-Degree System

Table VI. Coefficients of the Fourier Series Expansion

1	2	3	4	5	6	7	8	9
n	$\frac{6}{7}n\pi$	cos ②	sin ②	$\frac{7}{n\pi}$	④ · ⑤	③ + ⑥	$\frac{2}{n\pi}$	$\frac{bn}{po}$
1	154.29	-0.900	0.433	2.23	0.970	0.07	0.639	0.045
2	308.58	0.623	-0.783	1.11	-0.87	-0.247	0.317	-0.079
3	462.87	-0.223	0.975	0.743	0.72	0.497	0.212	0.105
4	617.16	-0.223	-0.975	0.558	-0.55	-0.773	0.159	-0.124
5	771.45	0.782	0.624	0.446	0.28	1.162	0.127	0.151
6	925.74	-0.900	-0.433	0.372	-0.16	-1.060	0.106	-0.113
7	1080.03	1.000	0.000	0.318	0.00	1.000	0.091	0.091
8	1234.32	- .0900	0.433	0.279	0.12	-0.780	0.080	-0.063

Note: Numbers in circle refer to the mathematical expression given in corresponding columns.

and substituting (52) and (53) into the differential equation of motion

$$M\ddot{x} + Rx = f(t),\qquad(54)$$

the unknown amplitudes X_n have been obtained from

$$X_n = \frac{f(t)}{(R - n^2 M)\,\sin nt}.\qquad(55)$$

The maximum displacement was $x_{max} = 0.24$ ft while the rigorous solution to the problem[32] yielded $x_{max} = 0.28$ ft, which is close enough for all practical purposes. If desired, a closer agreement can be achieved by using more terms and larger expansion period $(T \geq 15\ t_0)$.

The convergence of the membrane part of the stiffness coefficients has been tested using a deep beam problem (Figure 26) which was compared with the rigorous solution obtained by Timoshenko.[33] The convergence of the bending part of the stiffness coefficients was checked against a plate problem (Figure 27) with a known exact solution.[19] In both cases the solutions have shown monotonic convergence towards numbers close to the exact ones. Although the subdivisions in both cases could be considered relatively coarse, the discrepancy between exact and discrete element solutions was of negligible order of magnitude for practical purposes.

The free vibration of a cylindrical shell shown in Figure 28 has been computed, yielding, $\omega = 1.19 \times 10^4$ rad/sec for the lowest natural frequency, while the rigorous solution of this problem has yielded $\omega = 1.64 \times 10^4$ rad/sec. The discrepancy was caused mostly by the use of "lumped" mass matrix, which as discussed earlier, may cause one order of magnitude error. The second cause of discrepancy is the neglect of curvature effects, which will be treated in detail in the Section XII. Static loadings have yielded more favorable results.
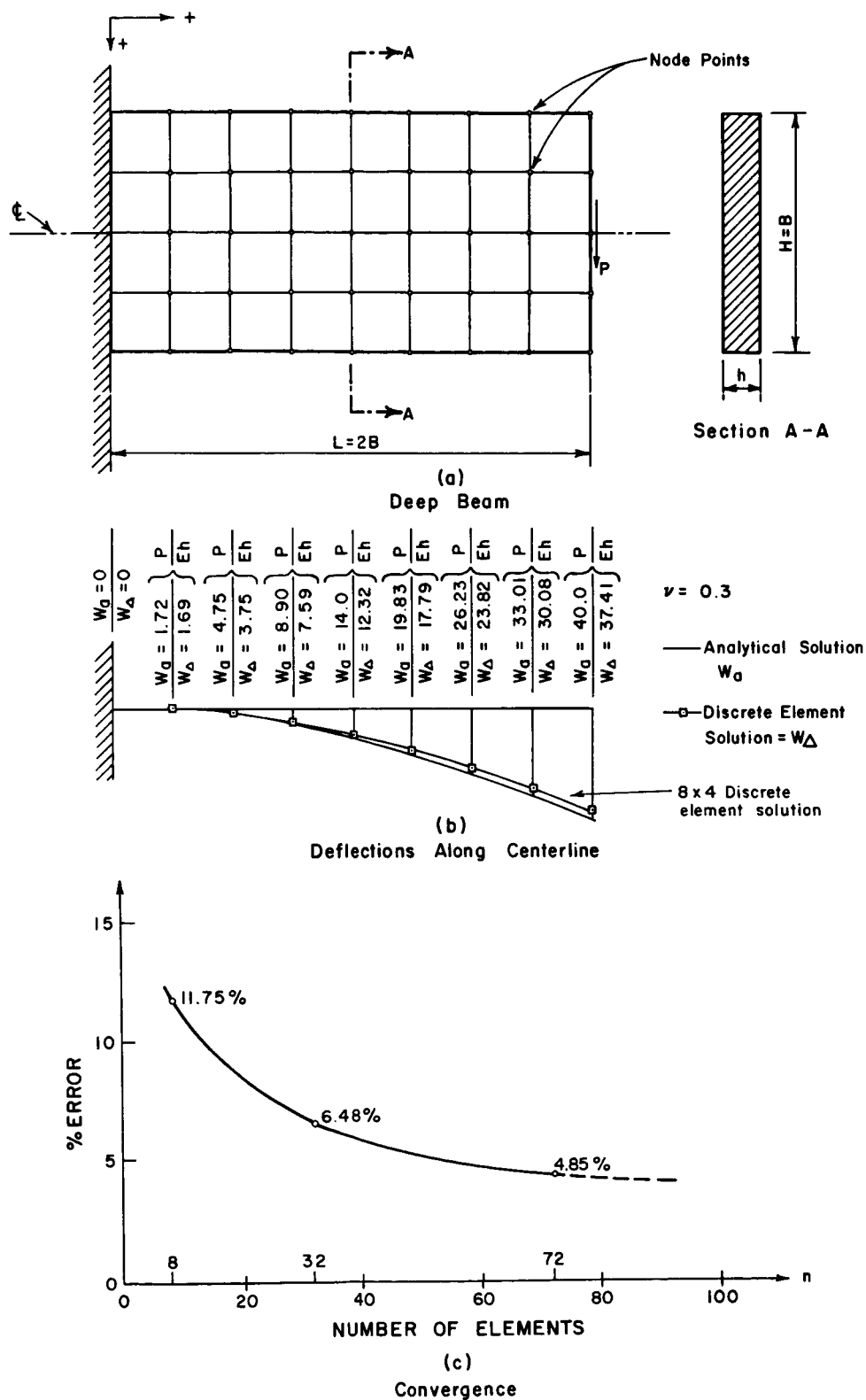
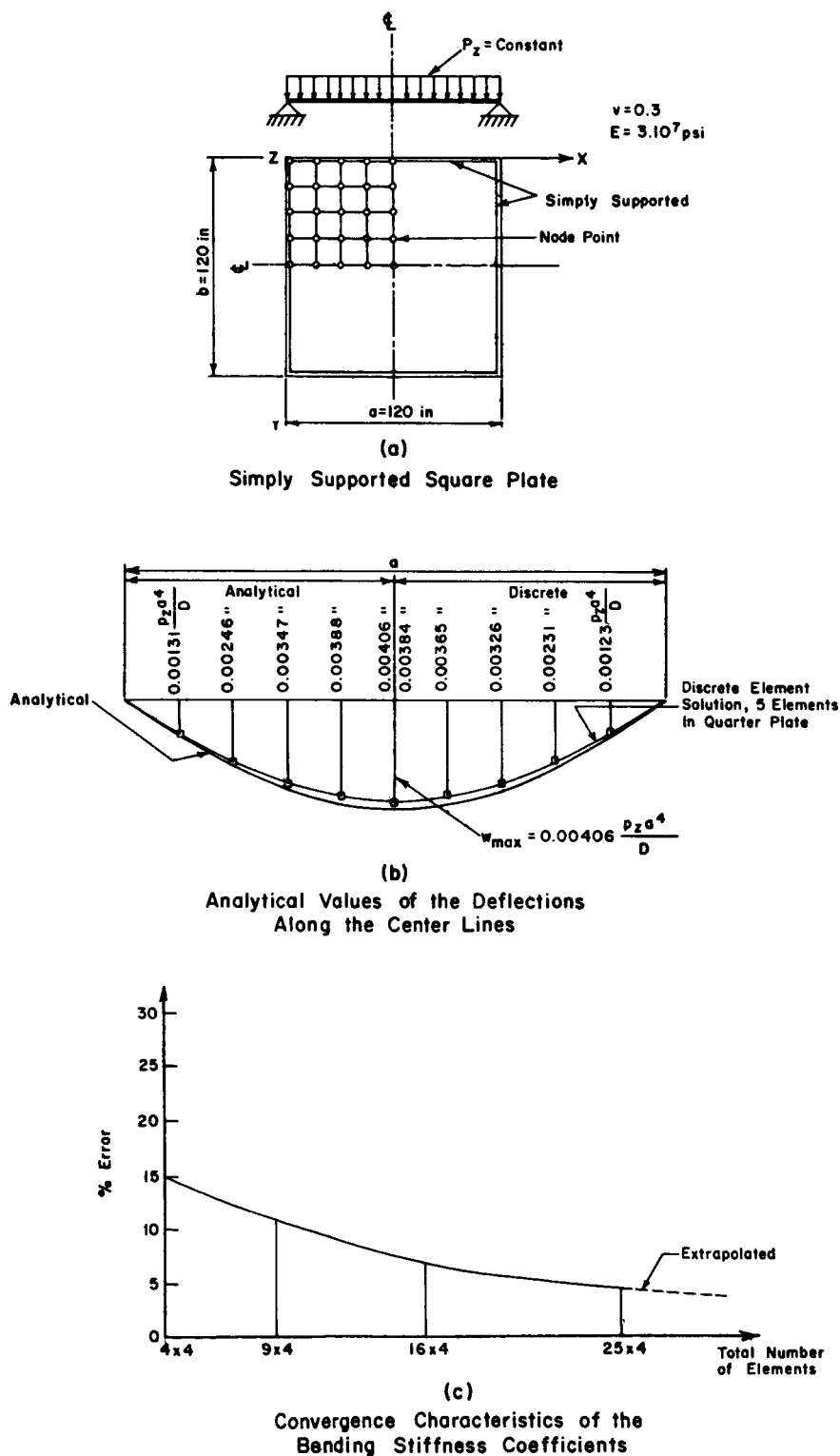Figure 26. Solution of a Deep Beam Problem

(a)
Simply Supported Square Plate

(b)
Analytical Values of the Deflections
Along the Center Lines

(c)
Convergence Characteristics of the
Bending Stiffness Coefficients

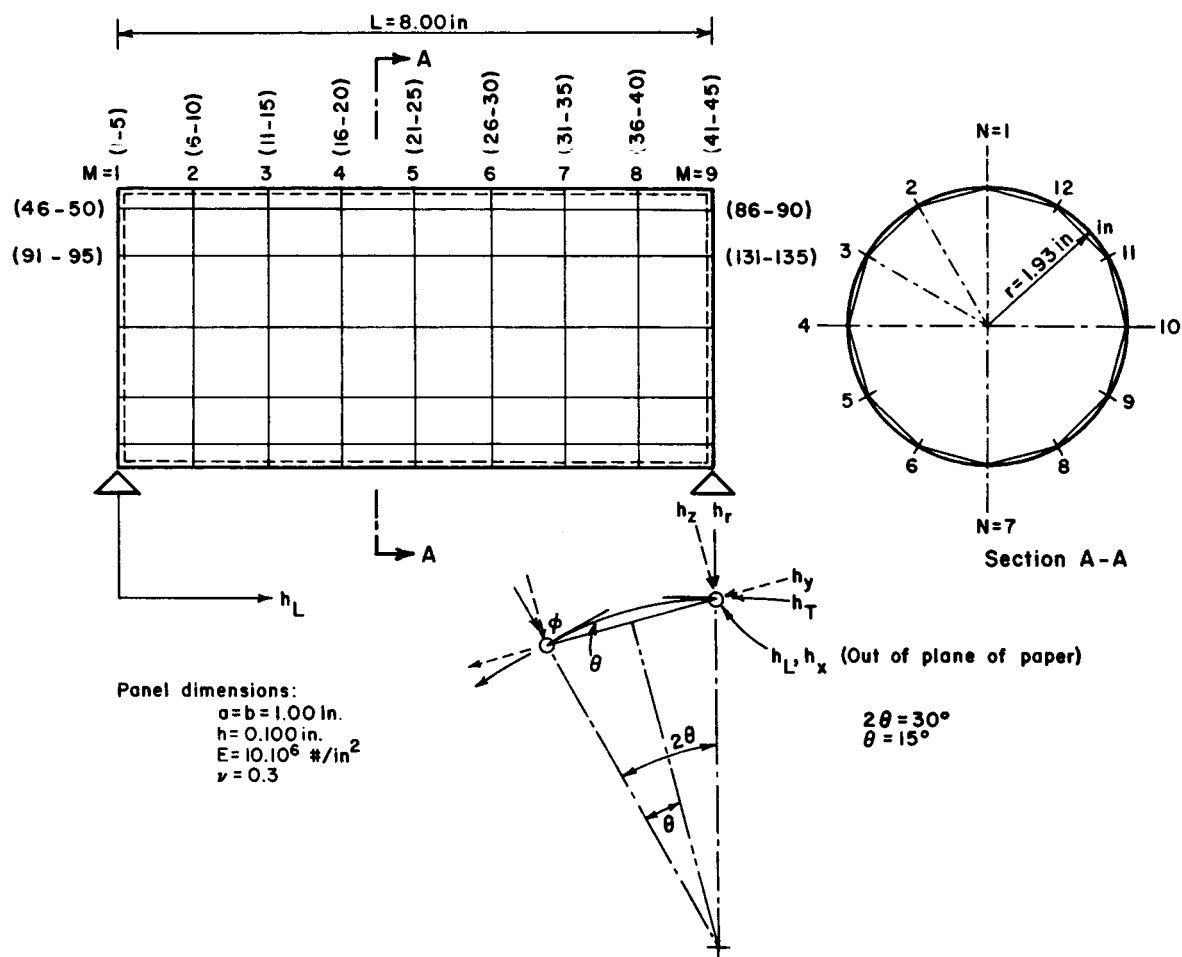Figure 27. Solution of a Plate Problem

Figure 28. Cylindrical Shell

XII.   THE EFFECT OF CURVATURE

Introducing curved elements instead of the flat ones, the previously derived stiffness coefficients of the element must be augmented by a "curvature term":

$$\rho_{ij} \text{ (curved)} = \rho_{ij}^{I} \text{ (flat)} + \rho_{ij}^{II} \text{ (curvature effect)}. \tag{56}$$

To derive exact values for the curvature effect, considerable effort is required, which was beyond the scope of this research. However, preliminary computations have been carried out to establish the order of magnitude of the curvature effects. For this purpose the similarity which exists between the differential equation of plates on elastic foundation and that of thin shallow shells has been utilized.

If $k_x = k_y = k$, the differential equation of thin shallow shell can be written as

$$\nabla^2 \nabla^2 w + \frac{12(1-\nu^2)\, k^2}{h^2}\, w = \frac{p_z}{D}, \tag{57}$$

while the differential equation of equilibrium of thin plates on elastic foundation has the form of

$$\nabla^2 \nabla^2 w + \frac{c}{D}\, w = \frac{p_z}{D}, \tag{58}$$

where c is the "bedding" constant.

The comparison of equations (57) and (58) yields

$$c = k^2 Eh \tag{59}$$

The lateral deflection $w(x, y)$ was computed using Galerkin's method,[19] in combination with method of images as shown in Figure 14.

The total energy of the plate of $2a \times 2b$ dimensions can be expressed as:

$$\int_0^{2a} \int_0^{2b} (D \nabla^2 w + c w)\ \delta w\ dx\, dy = P_2\ \delta w. \tag{60}$$

The deflection w(x, y) has been represented in form of series:

$$w(x, y) = A_1 f_1 (x, y) + A_2 f_2 (x, y) + \ldots A_r f_r (x, y), \qquad (61)$$

in which the functions f_1, $f_2 \ldots f_n$ were chosen in form of

$$f_r = \frac{1}{4} (1 - \cos \alpha_m x)(1 - \cos \beta_m y), \qquad (62)$$

where

$$\left. \begin{array}{l} \alpha_m = \dfrac{m\pi}{a} \quad ; \quad \beta_m = \dfrac{n\pi}{b} \\[2ex] m = 1, 3, 5 \ldots \quad n = 1, 3, 5 \ldots \end{array} \right\} . \qquad (63)$$

After obtaining the deflection due to $P_z = 1$ lateral loading acting at x = a and y = b, the deflections of the node points have been normalized as previously described.

The results of this computation for two arbitrary curvatures are shown in Figure 29 indicating a marked increase in the concentrated lateral load required to produce unit translation of the node as curvature increases.[34]

Similar computations have indicated an increase in the generalized moments producing unit rotation at the node point as curvature has been increased (Figure 30).

It is evident from this preliminary investigation that the curvature effects can change the stiffness coefficients up to 10% → 20%, thus their consideration is highly recommended if high accuracy should be obtained.

Another, probably more important reason for the introduction of curved elements instead of flat ends, comes from the previously discussed violation of slope compatibility at the adjoining edges. When flat plate idealization creates significant angles between elements the customary neglect of the in-plane rotation stiffness properties of the discrete elements is unjustified; whereas, in case of curved elements, the slope continuity is more completely satisfied, thus the effect of in-plane rotation is minimized.
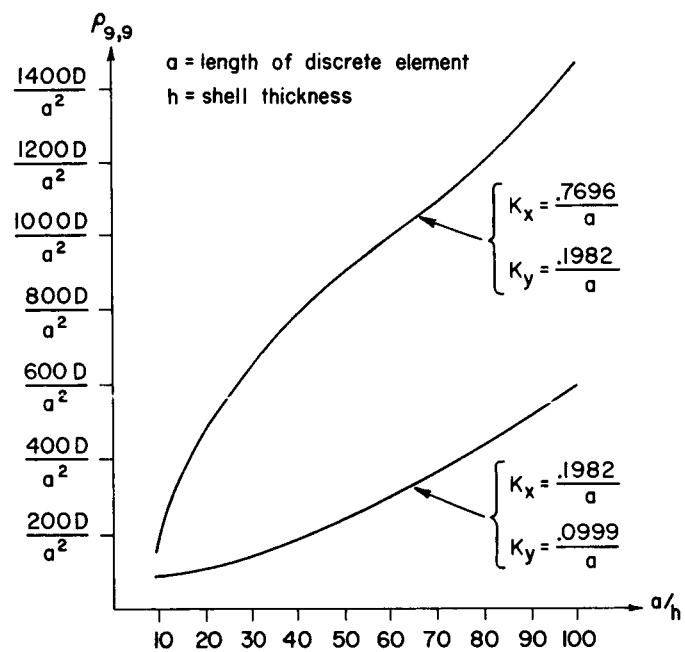
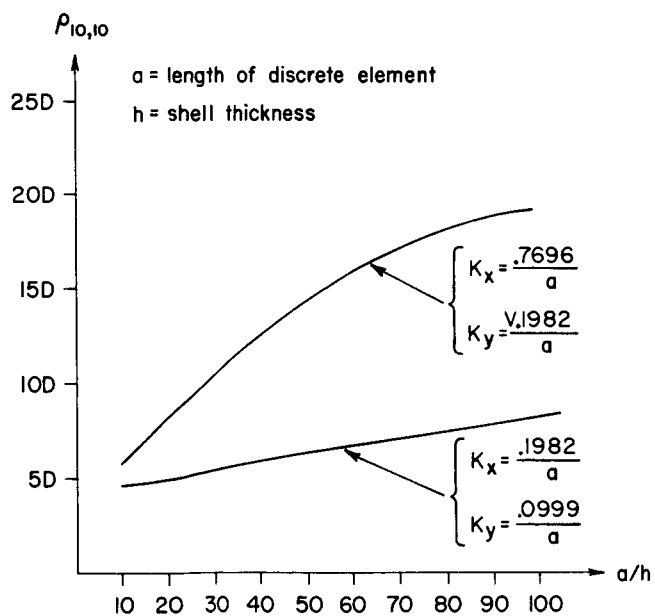Figure 29. Lateral Force Required for Unit Lateral Translation of Node vs. a/h Ratio

Figure 30. Bending Moment Required for Unit Rotation of Node vs. a/h Ratio

XIII. FUTURE DEVELOPMENTS

Although discrete element method for determination of static and dynamic response of shells is still in its infancy, the obtained results are highly encouraging. Future development should cover the two equally important areas: (a) improvement of stiffness matrices, and (b) solution of problems inherent to operation with large matrices.

In the field of improvement of stiffness matrices, the present research has indicated positive need for:

1. Introduction of various aspect ratios a/b.

2. Development of stiffness coefficients for triangular curved elements having various aspect ratios.

3. Derivation of readily usable coefficients for consistent mass matrices.

4. The use of symmetry and/or the method of substructures to reduce the order of stiffness matrix for free vibration problems.

5. Derivation of improved stiffness coefficients for the solution of three-dimensional stress problems in elastic continuum.

6. Stiffness coefficients for determination of thermo-stresses.

7. Extension of the stiffness matrix solution into non-linear regions covering (a) geometrical, and (b) material non-linearities.

8. Derivation of stiffness coefficients for thick shells.

9. Use of large elements.

10. Verification of analytical results, by experiments.

Future pertinent research and development in the field of mathematical and computer support should include:

1. Development of computer programs for inversion of large $(n \geq 1500)$ matrices.

2. Eigenvalue and eigenvector solution of large matrices.

3. Computers with larger storage capacity.

Prior to any large scale research funding of methods for the computer solutions of large matrix systems (inversion and eigenvalue-eigenvector programs), a study should first be made of the computer industry to determine their forecasts for computing time, machine storage and equipment costs over the next few years. Sufficient time and manpower has been spent in developing programs for standard hardware systems (32 k) over the last few years, that only minimal advances are being made at present. It should be understood that as these programs are being developed they are simultaneously being made obsolete by hardware advances in the computer industry.

Considerable part of the above listed required improvements are currently under study at Denver Research Institute for the Flight Dynamics Laboratory of the Air Force, Dayton, Ohio. [24]

XIV. CONCLUSIONS

The research described in this report has shown the feasibility of discrete element approach to complex static and dynamic shell problems. The cumbersome solution of complex differential equations inherent to problems of this nature has been eliminated and replaced by solution of simultaneous algebraic equations for which high speed electronic computers are primarily suited.

The key to the matrix solution of complex static and dynamic shell problems is the derivation of suitable stiffness coefficients. Thus new, improved compatible stiffness coefficients have been developed for flat plate elements and the effect of curvature has been briefly studied. The method applied is highly expandable and all stress problems can be handled with basically the same approach. It follows an approach which is familiar to structural engineers, rather than that of structural researchers, regardless of the complexity of the problem. Although the numerical computation of proper stiffness coefficients has been found to be a tedious operation, the results are reusable and can be furnished by researchers to the practicing engineer.

Limitations of the method along with the proposed improvements have been treated.

The author believes that the discrete element method will eventually replace all classical and semi-classical methods presently used by the designers for analysis of static and dynamic stress problems in one, two and three dimensional structures. Consequently the designer will be able to concentrate more on the "creative" aspects of the design leaving the tedious computations to the computers.

ACKNOWLEDGEMENTS

REFERENCES

1. Flügge, W., "Statik and Dyamik der Schalen," Second Edition, Springer-Verlag, Berlin, 1957.

2. Oniashvili, O. E., "Certain Dynamic Problems of the Theory of Shells" (in Russian), Press of the Academy of Sciences of USSR, Moscow, 1957.

3. Melosh, R. J., "Basis for Derivation of Matrices for the Direct Stiffness Method," AIAA Journal, Vol. 1, pp. 1631, 1963.

4. Szilard, R., "Analysis of Large-Span Shells of Arbitrary Shape Considering Geometrical and Material Non-Linearities," Paper to be presented at the International Symposium on Large-Span Shells to be held in Leningrad, September 1966.

5. Love, A. E. H., "A Treatise on the Mathematical Theory of Elasticity," Fourth Edition, Dover Publications, New York 1944.

6. Flügge, W., "Handbook of Engineering Mechanics," McGraw Hill Book Co., New York, 1962.

7. Soare, M., "Application des equations aux differences finites au calcul del coques," Editions Eyrolles, Paris, 1962.

8. Szilard, R., and West, A., "Survey of the State-of-the-Art of Dynamic Analysis of Shells of Arbitrary Shape, Including Thick Layered Orthotropic Shells," Denver Research Institute Report No. 560-6508-SP, August 1965.

9. Hrennikoff, A., "Solution of Problems of Elasticity by Framework Method," Journal of Applied Mechanics, December 1941.

10. Turner, M. J., Clough, R. W., Martin, H. C., Topp, L. J., "Stiffness and Deflection Analysis of Complex Structures," Journal of Aeronautical Sciences, September 1956.

11. Argyris, J. H. and Kelsey, S., "Modern Fuselage Analysis and the Elastic Aircraft," London, Butterworth Co., 1963.

12. Wehle, L. B. and Lansing, W., "A Method for Reducing the Analysis of Complex Redundant Structures to Routine Procedure," Journal of the Aeronautical Sciences, Vol. 19, October 1952.

13. Melosh, R. J., "Basis for Derivation of Matrices for the Direct Stiffness Method," AIAA Journal, July 1963.

14. Clough, R. W. and Tocher, J. L., "Finite Element Stiffness Matrices for Analysis of Plate Bending," Paper presented at the Conference on Matrix Methods in Structural Mechanics, October 26-28, 1965, Wright-Patterson Air Force Base, Ohio.

15. Born, J., "Faltwerke," Verlag Konrad Wittwer, Stuttgart, 1964.

16. Szilard, R., "A Matrix and Computer Solution of Cylindrical Shells of Arbitrary Shape," Proceedings of the International Symposium on Shell Structures in Engineering Practice, Budapest, 1965.

17. Hurty, W. C. and Rubinstein, M. F., "Dynamics of Structures," Prentice Hall, Englewood Cliffs, New Jersey, 1964.

18. Zurmühl, R., "Matrizen and ihre techischen Anwendungen," Springer-Verlag, Berlin, 1961.

19. Timoshenko S. and Woinowsky-Krieger, S., "Theory of Plates and Shells," Second Edition, McGraw-Hill Book Co., New York, 1959.

20. Wlassow, W. S., "Allgemeine Schalentheorie and ihre Anvendung in der Technik," Akademie-Verlag, Berlin, 1958.

21. Harold C. Martin, "Introduction to Matrix Methods of Structural Analysis," McGraw-Hill Book Co., New York, 1966.

22. Szilard, R. and Hubka, W. F., "Static and Dynamic Analysis of Plates of Arbitrary Shape and Boundary Condition," Publications Vol. 25, of the International Assoc. for Structural and Bridge Engineering, Zürich, 1965.

23. Apeland, K., "Analysis of Bending Stresses in Translational Shells Including Arisotropic and Inhomogeneous Properties," Acta Polytechnica Scandinavica, Civil Engineering and Building Construction Series, No. 22, Trondheim, 1963.

24. Szilard, R., and West, A. S., "Finite Curved Shell Elements and Consistent Mass Matrices for Static and Dynamic Analysis of Aerospace Structures," Air Force Technical Report (in preparation).

25. Flügge, W., "Stresses in Shells," Springer-Verlag, Berlin, 1960.

26. Taig, I. C., "Automated Stress Analysis Using Substructures," Paper presented at the Conference on Matrix Methods in Structural Mechanics, October 26-28, 1965, Wright-Patterson Air Force Base, Ohio.

27. Przemieniecki, J. S., "Matrix Structural Analysis of Substructures," AIAA Journal, January 1963.

28. Szilard, R., "Derivation of Compatible Stiffness Matrices for Large Discrete Elements" (in preparation for AIAA Journal).

29. Gallagher, R. H., "Techniques for the Derivation of Element Stiffness Matrices," AIAA Journal, June 1965.

30. Archer, J. S., "Consistent Mass Matrix for Distributed Mass Systems," Journal of the Structural Division, ASCE, August 1963.

31. West, A., "A Survey of Available Digital Computer Procedures for Inverting and Finding the Eigenvalues and Eigenvectors of Large Matrices with Adaptations to Accommodate Current Structural Research," Denver Research Institute Report No. 618-65-6-F, 1965.

32. Norris, C. H., Hansen, R. J., et al., "Structural Design for Dynamic Loads," McGraw-Hill Book Co., New York, 1959.

33.   Timoshenko, S. and Goodier, J. N., "Theory of Elasticity,"
       McGraw-Hill Book Co., New York, 1951.

34.   Edwards, J. C., "An Approximate Consideration of the Effect
       of Curvature on the Stiffness Coefficients of Finite Elements,"
       M. S. Thesis, University of Denver, July 1966.